International Journal of Nanomedicine

Dovepress
open access to scientific and medical research

Open Access Full Text Article

ORIGINAL RESEARCH

# Synergistic Nanocomposites of Different Antibiotics Coupled with Green Synthesized Chitosan-Based Silver Nanoparticles: Characterization, Antibacterial, in vivo Toxicological and Biodistribution Studies





This article was published in the following Dove Press journal:
*International Journal of Nanomedicine*

Muhammad Arif Asghar[1]
Rabia Ismail Yousuf[1]
Muhammad Harris Shoaib[1]
Muhammad Asif Asghar[2]
Sabah Ansar[3]
Mehrukh Zehravi[4]
Ahad Abdul Rehman[5]

[1]Department of Pharmaceutics, Faculty of Pharmacy and Pharmaceutical Sciences, University of Karachi, Karachi 75270, Pakistan; [2]Food and Feed Safety Laboratory, Food and Marine Resources Research Centre, PCSIR Laboratories Complex, Karachi, Sindh 74200, Pakistan; [3]Department of Clinical Laboratory Sciences, College of Applied Medical Sciences, King Saud University, Riyadh 11433, Saudi Arabia; [4]Department of Clinical Pharmacy, College of Pharmacy for Girls, Prince Sattam Bin Abdulaziz University, Al-Kharj 16278, Kingdom of Saudi Arabia; [5]Department of Pharmacology, Faculty of Pharmacy, Jinnah Sindh Medical University, Karachi 75510, Pakistan

Correspondence: Rabia Ismail Yousuf; Muhammad Harris Shoaib
Department of Pharmaceutics and Bioavailability and Bioequivalence Research Facility, Faculty of Pharmacy and Pharmaceutical Sciences, University of Karachi, Karachi 75270, Pakistan
Email rabia_pharmaceutics@yahoo.com; harrisshoaib2000@yahoo.com

**Purpose:** The present study reports chitosan functionalized green synthesized CS-AgNPs, conjugated with amoxicillin (AMX), cefixime (CEF), and levofloxacin (LVX) for safe and enhanced antibacterial activity.

**Methods:** The CS-AgNPs and conjugates CS-AgNPs+AMX CS-AgNPs+CEF, and CS-AgNPs+LVX were characterized by UV–Vis, FTIR, SEM, TEM, EDX spectroscopy. The size distribution and zeta potential were measured using the dynamic light scattering (DLS) technique. The interaction between CS-AgNPs and antibiotic molecules was also investigated using UV–Vis spectroscopy at the concentrations of 5, 50, 500, and 5000 µM for each antibiotic. Antibacterial activity and synergism were assessed by the Fractional Inhibitory Concentration (FIC) index. The mechanism for synergistic activity was investigated by the detection of hydroxyl species based on the chemiluminescence of luminol. The biocompatibility index (BI) was calculated from $IC_{50}$ using the HeLa cell line. In vivo toxicity and tissue distribution of silver ions were evaluated on Sprague Dawley rats. Physical interactions of antibiotics and significant ($P<0.05$) antibacterial activity were observed after loading on CS-AgNPs surfaces.

**Results:** The spherical shape nanocomposites of CS-AgNPs with different antibiotics were prepared with mean size ranges of 80–120 nm. $IC_{50}$ of antibiotics-conjugated CS-AgNPs decreased compared to CS-AgNPs. The biocompatibility (BI) index showed that antibiotics-conjugated CS-AgNPs have high antibacterial potential and low toxicity. Highly significant ($P<0.005$) increase in the generation of hydroxyl species indicated the radical scavenging mechanism for synergistic activity of CS-AgNPs after combined with different antibiotics. Biochemical analysis and histopathological examinations confirmed low toxicity with minor hepatotoxicity at higher doses. After oral administration, extensive distribution of Ag ion was observed in spleen and liver.

**Conclusion:** The study demonstrates positive attributes of antibiotics-conjugated CS-AgNPs, as a promising antibacterial agent with low toxicity.

**Keywords:** chitosan functionalized silver nanoparticles, antibiotic resistance, synergistic antibacterial activity, in vivo toxicity, tissue distribution

## Introduction

The convergence of nanotechnology with nanomedicine has brought new hope to the pharmaceutical and therapeutic fields. Today, nanoparticles (NPs) have been used as diagnostic agents, fluorescent labels, antimicrobial agents, and transfection

labels.[1,2] Silver nanoparticles (AgNPs) have unique physicochemical and biological characteristics with the high surface area due to the variable size ranges from 1 to 100 nm.[3] These unique characteristics of AgNPs have attracted globally and are considered a potent antimicrobial agent. It has been suggested that silver NPs has a significant antimicrobial activity due to multiple reasons including their high affinity with the surface active groups of microbial strains, released of silver ions can rapture the bacterial cell wall or distortion of bacterial DNA helical structure.[4,5]

At recent times, natural polysaccharides have been widely used in numerous medical fields such as drug delivery, electrochemical devices, cell imaging, energy storage and biosensors.[6–8] Especially, chitosan (CS) a carbon-based natural polymer, is one of the non-toxic, biocompatible, and cost-effective raw biomaterial, majorly found in crustaceans.[9] CS has been a widely used biological macromolecule as a drug carrier in the pharmaceutical sector. Previously, researchers reported the antimicrobial activity of CS as nanocarrier.[10,11] CS is non-toxic, a biodegradable natural polysaccharide with intrinsic antibacterial activity. It has an $NH^{3+}$ group in its structure can adsorb on a cell wall by electrostatic interaction.[12] It also reduces the need for additional reductant while conjugation with silver nanoparticles.[13]

The worldwide increase in mortality and morbidity rates due to multi-drug resistant pathogenic bacterial strains poses a severe challenge in the field of medicines. The World Health Organization (WHO) reported that more than 64% of patients die due to methicillin-resistant *Staphylococcus aureus* (MRSA) infections compared to non-resistant bacterial infected patients.[14] The irrational use of antibiotics is the root cause of the development of resistance by bacterial strains against various antibiotics.[15]

To combat the multi-drug resistance crisis, novel approaches should be applied to bring improvements in current treatment options. Many researchers worked on the synergism of antibiotics using different non-toxic and eco-friendly techniques. Recently, several studies reported the synergistic antibacterial activities of different antibiotics after combinations with different metallic nanoparticles.[16–20] Some studies have described the reduction in the cytotoxicity of antimicrobial compounds after conjugations.[21,22] However, the potential in vivo toxicity and tissue distribution of these synthesized and conjugated silver nanoparticles have not yet been investigated. Similarly, no report has been found for the assessment of synergism, in vivo toxicity and tissue distribution of chitosan functionalized silver nanoparticles (CS-AgNPs), synthesized from an extract of *Syzygium aromaticum* (clove bud).

The exponential rise in antimicrobial resistance is a big everyday challenge faced by clinicians. To combat the crisis, novel combinations of green synthesized silver nanocomposites, functionalized with chitosan, and conjugated with antibiotics, have been developed in the current study. The work is focused on evaluating the toxicity and antibacterial effectiveness of these synergistic combinations. Moreover, histopathological evaluation and bio-distribution of silver ion in different doses of CS-AgNPs, by atomic absorption technique were also performed.

## Materials and Methods

### Antibiotics Loading on Synthesized Chitosan Based Silver Nanoparticles (CS-AgNPs) Surfaces

Green synthesis of AgNPs using *Syzygium aromaticum* ethanolic extract (SAEE) and functionalized with chitosan (CS-AgNPs) was described in our previous study.[23] Briefly, AgNPs were synthesized by adding SAEE (10 mol%) dropwise to the $AgNO_3$ (1 mmol/L) solution in the ratio of 9:1. At room temperature, the mixture was continuously stirred and left in a darkroom for 24 h to prevent photodegradation of silver ions. Then, the obtained suspension was centrifuged at 10,000 rpm for 40 min. After centrifugation, supernatant was drawn, washed with distilled water and assess on UV spectrophotometer for AgNPs synthesis. Moreover, the change in color from silver to brownish-black was also indicated the completion of AgNPs synthesis. Finally, the synthesized AgNPs were dried at 65°C for 3 h in a hot air oven. However, functionalization of chitosan with AgNPs was done by dissolving 0.5 g of CS in an acetic solution, and then 0.1 g of AgNPs was added in the prepared CS solution with constant stirring for 45 min. The synthesized precipitate of CS-AgNPs was washed, centrifuged at 10,000 rpm for 10 min, and then dried at 65°C for 12 h in a hot air oven to obtain a purified nanocomposite of CS-AgNPs.

Ten milliliters of 10 µg/mL of synthesized CS-AgNPs was added to the selected widely prescribed antibiotics, ie, amoxicillin (AMX) (25 µg/mL), cefixime (CEF) (5 µg/mL) and levofloxacin (LVX) (5 µg/mL) in the presence of 2-(N-morpholino) ethane sulfonic acid buffer. The solution

was stirred using a magnetic stirrer at ambient temperature for 45 min, and surface plasmon resonance (SPR) fluctuation was monitored using a UV spectrophotometer. The nanocomposites of CS-AgNPs after conjugation with different antibiotics were washed with distilled water, filtered, and then dried at 65°C in an oven for 12 h. The efficiency of antibiotics loading on CS-AgNPs was evaluated by measuring the supernatant residues of antibiotics using a UV spectrophotometer after centrifugation at 14,000 rpm for 15 min.[24] The antibiotics loading were calculated by Eq. 1:

$$\text{Antibiotic (AB) loading efficiency (\%)} = \frac{\textit{Total amount of AB} - \textit{Amount of supernatant AB}}{\textit{Total amount of AB}} \times 100 \quad \text{(Eq. 1)}$$

## Characterization and Interaction of Antibiotics Loaded on CS-AgNPs Surfaces

UV visible spectrophotometer (Shimadzu, Model no: UV-1712, Japan) was used to evaluate the optical properties of antibiotics-loaded CS-AgNPs at the wavelength range of 200–700 nm. Field emission scanning electron microscope (FESEM; Joel, Model no: JSM 4380B, Japan) and transmission electron microscope (TEM; Joel, Model no: JEM 300F, Japan) were used to assess the size and surface morphology of antibiotics-loaded nanocomposites. Fourier-transform infrared spectroscope (FTIR; Shimadzu, Model no: IR-100, Japan) in the operational wavelength of 500–4000/cm and energy dispersion x-ray spectroscope (EDX; Joel, Model no: JSM 6360, Japan) within 0 and 10 kV range, were used to identify the presence of functional groups and silver ions in antibiotics-loaded CS-AgNPs, respectively. The size distribution and stability of green synthesized AgNPs, CS-AgNPs, and antibiotics conjugated nanocomposites were analyzed using dynamic light scattering (DLS) technique along with a particle size analyzer (Brookhaven, USA).[24,25] The interaction of CS-AgNPs with the studied antibiotics was investigated by the addition of each antibiotic separately to CS-AgNPs solution (50 µM). The CS-AgNPs/antibiotic ratio varied with the concentration of the antibiotic from 5 to 5000 µM. The UV/Vis spectrums were recorded after mixing for 2 h at different concentrations.[26] Also, the mass of each nanocomposite was estimated after dried in a hot air oven at 65°C while proper concentrations of AgNPs, CS, and different antibiotics in each nanocomposite were determined by dissolving each nanocomposite in deionized water and estimated on UV spectrophotometer.

## Antibacterial Activity of AgNPs, CS-AgNPs and Antibiotics-Loaded NPs

### Zone of Inhibitions (ZIs)

Pathogenic bacterial strains of *Escherichia coli* (LT 01253), *Klebsiella pneumoniae* (LT 0471), *Staphylococcus aureus* (LT 3512), *Salmonella typhi* (LT 01057), and *Pseudomonas aeruginosa* (LT 0261) were obtained from Kutiyana Memorial Hospital Laboratory Karachi – Pakistan. The in vitro antibacterial activity of SAEE, CS, AgNPs, CS-AgNPs, and antibiotics-loaded NPs were analyzed using the Oxford cup well diffusion method.[27] The concentration of each bacterial strain was made equivalent to ($10^6$ CFU/mL) as McFarland turbidity standard in nutrient broth. The bacterial suspension was spread, and 6 mm of sterile Oxford diffusion cups were placed on agar plates. Then, each antibacterial agent was dispensed in Oxford diffusion cups individually with the concentration of 10,000 µg/mL of SAEE, 1000 µg/mL of CS, 50 µg/mL of both AgNPs and CS-AgNPs, 25 µg/mL of AMX, 50+25 µg/mL of CS-AgNPs+AMX, 5 µg/mL of CEF, 50+5 µg/mL CS-AgNPs+CEF, 5 µg/mL of LVX and 50+5 µg/mL of CS-AgNPs+LVX. Plates were incubated for 24 h at 37 ± 2°C after 30 min diffusion period. The ZIs of each test solution were measured using a digital Vernier caliper and expressed in millimeter. ZIs determination was performed in triplicate.

The increase in antibacterial activity of each antibiotic (AB) after combination with synthesized CS-AgNPs was calculated using the following equation:

$$\text{Fold increase of ZI} = \frac{\textit{ZI of CS-AgNPs+AB} - \textit{ZI of AB}}{\textit{ZI of AB}} \quad \text{(Eq. 2)}$$

### Minimum Inhibitory Concentrations (MICs), Fractional Inhibitory Concentrations (FICs) Index, and Minimum Bactericidal Concentrations (MBCs)

In the current study, MICs of SAEE, CS, AgNPs, CS-AgNPs, and antibiotics-loaded CS-AgNPs were estimated using the broth dilution method.[28] The assay was performed at the concentration ranges of SAEE (1000 to 30,000 µg/mL), CS, AgNPs and CS-AgNPs (1 to 512 µg/mL) and antibiotics alone (0.016 to 1024 µg/mL) in nutrient broth. However, the concentrations of CS-AgNPs in combinations with antibiotics were tested using the checkerboard titration method.[21] Basically, a checkerboard titration method is normally used to assess two variables at

once: in our case, CS-AgNPs concentration and antibiotics concentration. By plating each strain with a different ratio of CS-AgNPs to an antibiotic, we found not only the optimal concentration of each but the optimal ratio of concentrations as well. All culture strains were adjusted to Mcfarland standard concentrations of $10^6$ CFU/mL. An optical density (ODs) of each plate was determined after incubation using the ELISA reader (Infinite 200; USA) at 600 nm. Each assay was performed three times and values are expressed in mean ± SD.

FIC index determination is an important tool for the assessment of synergism of different antibacterial agents. The concentrations of CS-AgNPs and antibiotics were used in the range of 2 x MICs to 1/16 x MICs for the determination of FICs. For calculation of the FIC index, the comparison was made between the MICs of the antibacterial agent alone and in combination derived MIC. FICs index equal to ≤0.5 demonstrates the synergistic activity of the combination used, while FICs in the ranges of 0.5–1, 1–4, and >4 are considered as an additive, indifferent and antagonistic combinations respectively.[29] FIC index was calculated using the following equation:

$$\mathrm{FIC} = \frac{MIC\ of\ CS-AgNPs\ combined\ with\ AB}{MIC\ of\ CS-AgNPs\ alone} + \frac{MIC\ of\ AB\ combined\ with\ CS-AgNPs}{MIC\ of\ AB\ alone} \quad (\text{Eq. } 3)$$

Minimum Bactericidal Concentrations (MBCs) were determined by spreading the 100 µL solution from already incubated tubes of each test sample on nutrient agar plates and incubated for 24 h at 37 ± 2°C. Then, bacterial colonies were observed after the incubation period.[21] The MBC is defined as the lowest concentration of test solution exhibiting complete (>99.9%) killing of a bacterial strain.[30]

### Mechanism of Synergistic Effects of CS-AgNPs in Combination with Different Antibiotics

The mechanism of synergistic activity of CS-AgNPs in combination with different antibiotics was evaluated by the assessment of hydroxyl radical generation using the luminol chemiluminescence method.[31] The production of hydroxyl radicals was evaluated by mixing 100 µL of luminol solution with 100 µL AgNPs and 2 µL of antibiotic water solution (40 mg/mL) to obtain a final concentration of 0.4 mg/mL for each antibiotic while combinations of these agents were used at their FICs. The measurement of chemiluminescence was done on a luminometer (LUMAT LB 9507) (Berthold Technologies) and noted in $sec^{-1}$(see Figure 5).

## Toxicity Studies

### In vitro Cytotoxic Evaluation of Antibiotics and Antibiotics-Loaded CS-AgNPs

The cytotoxic potential of antibiotics-loaded CS-AgNPs was evaluated in triplicate using the HeLa cell line (ATCC, Virginia, USA) assay. The percentage viability of cells was determined using MTT (3 (4,5 dimethyl thiazol 2) 2.5 diphenyltetrazolium bromide) assay, as reported in previous studies.[21,22] For the determination of $IC_{50}$, all antibiotics in the concentrations range of 0.016–1024 µg/mL were used, whereas CS-AgNPs conjugated with AMX, CEF, and VAX, were applied in the concentrations according to their respective FICs (defined in Table 3). Briefly, prior to the incubation for 24 h, each test solution was added separately in an adherent culture medium. Then, the cells were washed using phosphate-buffered saline (PBS) and again incubated for 30 min at room temperature in MTT reagent (1 mg/mL). After incubation, cell viability was assessed using a differential interference contrast microscope also with the help of UV spectrophotometer at 570 nm and the growth inhibition was expressed in percentages.

### Biocompatibility Index (BI) of CS-AgNPs, Antibiotics and Antibiotics-Loaded CS-AgNPs

The biocompatibility index is defined as the ratio of $IC_{50}$ values of test solution determined on HeLa cell line and concentration of test solution produced 3 $\log_{10}$ reductions of bacterial growth (99%). The BI values higher than "1" demonstrates that test solution has more bactericidal potential and low cytotoxicity, while lower than "1" indicates low bactericidal potential with high cytotoxic activity.[32] In this study, BI was determined using MBC values at which a 99.9% reduction in bacterial growth was observed.

### In vivo Acute- and Sub-Toxicity Studies of CS-AgNPs

#### Study Animals

For in vivo toxicity studies on an animal model, ethical approvals were obtained from the Institutional Bioethics Committee (IBC) of the University of Karachi, Karachi, Pakistan, and also from Institutional Review Board (IRB) of the Jinnah Sindh Medical University with the reference number of JSMU/IRB/2019/286. Healthy Sprague dawley rats (10–12 weeks old) of both genders were purchased

from the animal house of Dow University of Health Sciences. Animals were kept in a standard environment (45–55% humidity and 25°C ± 2°C) with a 12 h light-dark cycle.[33] They were divided into four groups, with 10 rats in each. All administrations were performed orally, and tested solutions were given once daily. Normal saline was given to 1st group (control) while 2nd, 3rd, and 4th test groups received 30 mg/kg, 60 mg/kg, and 90 mg/kg CS-AgNPs for 28 days, respectively. The test doses were adapted based on a preliminary acute toxicity study where a lethal dose ($LD_{50}$) was found to be >200 mg/kg using a staged approach to the dosing method.[34] T-61 agent was administered IV as euthanasia, while medetomidine was used for animal sedation.[35] Animal handling was performed according to the guidelines of the National Advisory Committee for Laboratory Animal Research (NACLAR). The toxicity studies were performed according to the Organization for Economic Corporation (OECD) guidelines no 407 and 425.[36]

### Clinical Examinations, Body Weight, and Relative Organ Weights

Initially, all test animals were evaluated for generalized well-being. After the dosing of CS-AgNP, the vital signs or any sign of toxic effects were recorded twice daily. Treatment effects on animal general health, behavior, hairs, and skin were observed. The body weight of each animal was noted on initial then after continued dosing for 28 days. Organ weights such as the brain, heart, kidney, liver, and lungs were measured and relative organ weights were calculated based on their total body weight.

### Hematological and Biochemical Analysis

Animals were anesthetized and then sacrificed after the last dosing. A volume of 5 mL of blood samples from each rat was collected from the femoral artery into the 20 mg/mL ethylenediaminetetraacetic acid (EDTA), which is used as an anticoagulant for hematological and biochemical analysis. Blood samples were analyzed for the counts of red blood cells (RBCs), white blood cells (WBCs), and differential WBCs using an automated blood sample analyzer (Beckman Coulter, U.S). Hemoglobin levels (Hb levels), serum electrolytes, erythrocyte sedimentation rate (ESR), and cholesterol levels were also estimated. The auto analyzer (7600–110, Hitachi, Japan) was used for biochemical analysis related to enzymatic levels of heart, liver, and kidney. Different inflammatory biomarkers, including C-reactive proteins, interleukins (IL)-1, IL-2, IL-6, IL-10, and tumor necrosis factor-alpha (TNF-α) were determined by MAGPIX (R&D Systems) in accordance with the manufacturer's instructions provided on commercial assay kits.[33,37]

### Histopathological Examination

Tissues of heart, kidney, and liver were fixed in formalin (10%), and tissues were handled using standard laboratory techniques recommended for histopathological examinations. Tissue cleaning was done using a xylene solution (1%) for 1 h. Then, 3 to 5 µm sections were sliced using a microtome and stained with hematoxylin-eosin (H&E) stain according to the standard protocol for staining.[38]

## Determination of Silver Ion Concentration in Tissues

Silver ion concentration was determined in different organs after the administration of CS-AgNPs in similar dosing scheduled used for toxicity studies according to the method reported by Lee et al in 2013.[37] The animals were sacrificed after 28 days, and tissues were digested in nitric acid using a multiwave microwave digester (Anton Paar, USA). The atomic absorption (AA) spectrophotometer (AA-7000, Shimadzu, Japan) equipped with a graphite furnace (Elmer, USA) was used for the Ag ion determination. The Ag ion concentration in each tissue was calculated in µg/g wet weight. The limit of detection (LOD) and the limit of quantification (LOQ) were found to be 0.29 µg/kg and 0.88 µg/kg, respectively, in the quantification method.

## Statistical Analysis

All results are presented as their mean ± S.D values. The synergistic antibacterial activity, in vitro and in vivo toxicity findings, and silver ion determination were subjected to analysis of variance (ANOVA), two-tailed *t*-test, and Tukey post hoc tests using SPSS software (version 23). $P< 0.05$ and $P< 0.005$ were considered statistically significant and highly statistically significant results, respectively.

# Results and Discussion

## Antibiotics Loading on Synthesized Chitosan-Loaded Silver Nanoparticles (CS-AgNPs) Surfaces

Amount and loading efficiencies of AMX, CEF, and LVX to CS-AgNPs were found to be 2.5 µg/µg (93.3%), 0.5 µg/µg (85.8%), and 0.5 µg/µg (82.0%) respectively, using

UV-Vis spectrometric analysis. UV-vis absorption peaks for AMX were obtained at 337 nm, for CEF at 321 nm and LVX at 292 nm with CS-AgNPs (Figure S1). The peaks of these antibiotics at similar wavelengths have also been reported by other researchers.[39–41]

## Characterization and Interaction of Antibiotics Loaded on CS-AgNPs Surfaces

The size, shape, and agglomeration of synthesized CS-AgNPs conjugated with antibiotics were evaluated by SEM and TEM analysis. SEM and TEM images are presented in Figure S2 and S3, respectively. Images showed more agglomeration in antibiotics-loaded NPs compared to AgNPs and CS-AgNPs alone, which may be due to the antibiotics conjugation on NPs surfaces.[25] For AgNPs and CS-AgNPs, absorption peaks at 2922/cm (hydrocarbon chains), 1647/cm (C–O), and 1382/cm (C–O–H stretching vibrations) correspond to the presence of organic compounds that prevent agglomeration.[42] FTIR spectra also confirmed the antibiotics were loading on CS-AgNPs surfaces, as reflected in Figure S4. Major absorption peaks observed at 3463/cm (N-H) and 3167/cm (O-H) while stretching vibrations of carboxylic group and amide groups were observed at 1775/cm and 1685/cm respectively, in CS-AgNPs+AMX spectra, indicating the conjugation of AMX with CS-AgNPs. Hovoofa[illegible] reported similar absorption peaks in the separation and characterization study of AMX [illegible]e.[43] IR spectra of CS-AgNPs+CEF displays the absorption peak of $NH_2$ at 3260/cm and at 1665/cm for the amide group while the absorption band for the carboxylic group at 1760/cm confirms the presence of CEF on CS-AgNPs surfaces.[44] Characteristics peaks at 1730/cm (C=O), 1888/cm (quinolone moiety), and 2940/cm (aromatic stretching) were observed for LVX in CS-AgNPs+LVX spectra corresponded with the absorption peaks of LVX reported by Khan et al in 2016.[45] EDX technique was used for the localized detection of silver metal in antibiotics-loaded CS-AgNPs. In Figure S5 absorption band peaks at 3 KeV, confirmed the presence of silver ion in antibiotics-loaded NPs in all EDX spectra.[45] The size distribution and zeta potential of the AgNPs, CS-AgNPs, and antibiotics-loaded CS-AgNPs were determined by [illegible]. The particle size distribution curve shows that obtained AgNPs and CS-AgNPs were monodispersed with the mean size ranges of 10–20 and 20–40 nm, respectively (Figure S6). However, polydispersion was observed in antibiotics-conjugated nanocomposites with an increase in mean size ranges from 80 to 120 nm, which might be due to the presence of non-specific binding and aggregation between antibiotics and NPs.[46] The measurements of zeta potential revealed that negative charge of green synthesized AgNPs and CS-AgNPs with the mean potential of −23.6 and −16.1 mV, respectively (Figure S7). The shifting of surface charges toward positivity was observed after conjugation with AMX and LVX with the mean zeta potential of −7.9 and −19.4 mV, respectively. Aggregation between antibiotics and AgNPs might be observed due to these

**Table 1** Zone of Inhibitions (mm) of Different Antibacterial Agents Against Clinical Isolates

| Antibacterial Agents | Zone of Inhibitions (mm ± S.D) | | | | |
|---|---|---|---|---|---|
| | *E. coli* | *K. pneumoniae* | *S. aureus* | *S. typhi* | *P. aeruginosa* |
| Control (Distilled water) | 0.00 ± 0.00 | 0.00 ± 0.00 | 0.00 ± 0.00 | 0.00 ± 0.00 | 0.00 ± 0.00 |
| SAEE | 7.1 ± 0.57 | 6.3 ± 0.38 | 6.2 ± 0.17 | 6.2 ± 0.36 | 8.3 ± 0.74 |
| CS | 9.6 ± 0.32 | 9.4 ± 0.47 | 8.8 ± 0.26 | 7.1 ± 0.20 | 11.4 ± 0.39 |
| AgNPs | 13.2 ± 0.41* | 12.3 ± 0.52* | 11.9 ± 0.22 | 9.4 ± 0.47 | 13.1 ± 0.68* |
| CS-AgNPs | 16.1 ± 0.83* | 15.2 ± 0.16* | 16.5 ± 0.54* | 15.3 ± 0.23* | 18.4 ± 0.30* |
| AMX | 11.4 ± 0.23 | 6.3 ± 0.36 | 9.8 ± 0.19 | 12.8 ± 0.61* | 11.8 ± 0.57 |
| CS-AgNPs + AMX | 21.5 ± 1.03** | 19.7 ± 0.67** | 23.6 ± 1.57** | 24.5 ± 0.90** | 26.2 ± 1.53** |
| CEF | 14.5 ± 0.54* | 17.6 ± 0.71* | 7.1 ± 0.15 | 14.8 ± 0.77* | 10.5 ± 0.24 |
| CS-AgNPs + CEF | 23.4 ± 0.35** | 26.8 ± 1.32** | 19.7 ± 0.97** | 23.5 ± 1.57** | 21.9 ± 1.07** |
| LVX | 16.0 ± 0.64* | 13.0 ± 0.74* | 15.3 ± 0.83* | 16.0 ± 0.24* | 17.9 ± 0.62* |
| CS-AgNPs + LVX | 25.5 ± 0.49** | 27.7 ± 1.26** | 29.4 ± 2.18** | 31.7 ± 2.80** | 32.5 ± 2.60** |

**Notes:** All experiments were performed in triplicates and reported as mean ± SD. *$p \leq 0.05$ significant as compared to control, **$p \leq 0.005$ highly significant as compared to control.

**Abbreviations:** S.D, standard deviation; SAEE, *Syzygium aromaticum* ethanolic extract; CS, chitosan; AMX, amoxicillin; CEF, cefixime; LVX, levofloxacin.

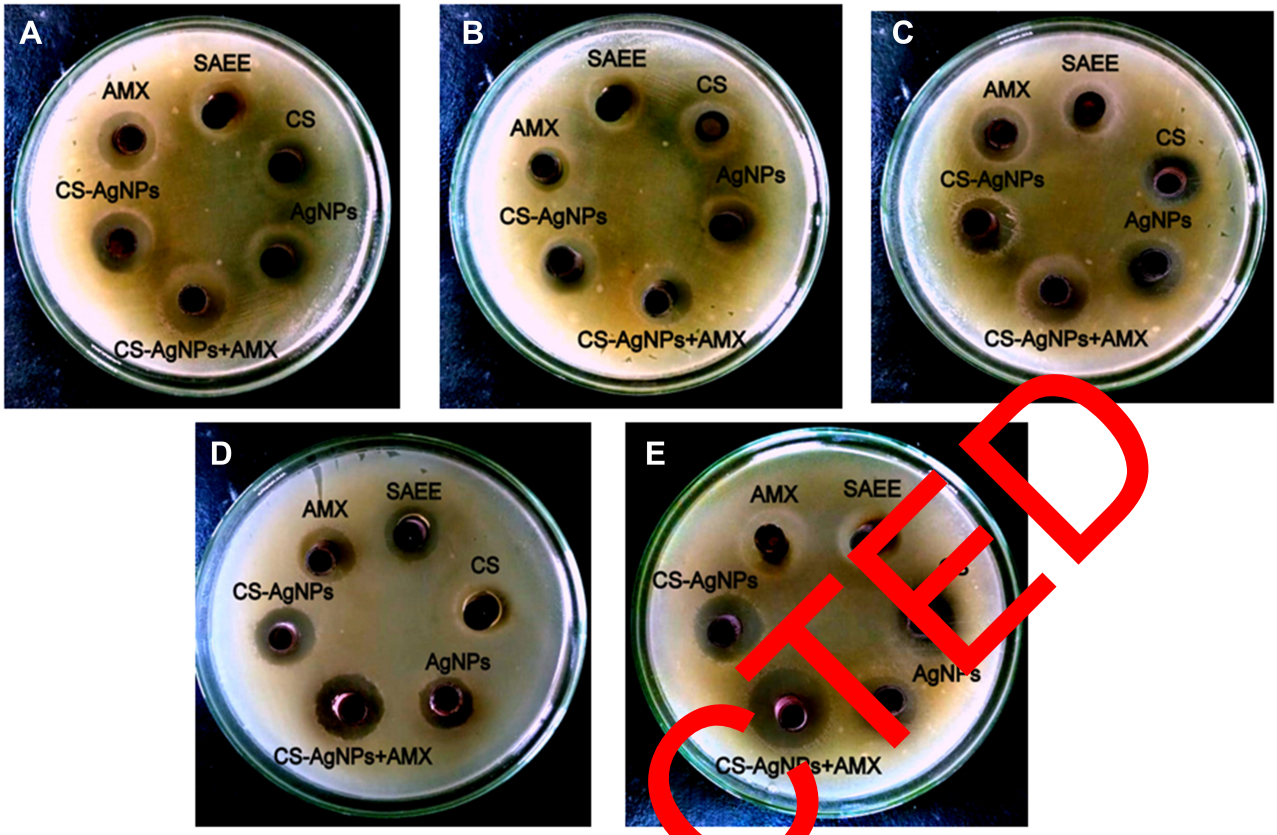


**Figure 1** Antibacterial activities of CS-AgNP with amoxicillin against (**A**) *Escherichia coli*; (**B**) *Klebsiella pneumoniae*; (**C**) *Staphylococcus aureus*; (**D**) *Salmonella typhi*; (**E**) *Pseudomonas aeruginosa*.



positive-negative charges attractions. However, the negative potential value after final conjugation with CEF (−34.4 mV) supports good colloidal nature, long-term stability and high dispersity of nanocomposites.[46]

UV/Vis spectroscopy was used to investigate the interaction between CS-AgNPs and individual antibiotic molecules. Upon addition of AMX, a slightly decreased in the extinction at 410 nm of CS-AgNPs in the entire concentration range from 5 to 5000 μM was observed, without significant aggregation of synthesized CS-AgNPs. However, the broadband dominates the spectrum when CEF or LVX concentrations gradually increased, and the aggregation of CS-AgNPs was observed at 500 and 5000 μM after the addition of LVX and CEF, respectively, as shown in Figure S8. This means that both antibiotics formed complexes physically with CS-AgNPs resulted in aggregation of the CS-AgNPs. This spectral information from UV-Vis spectrum clearly demonstrate that CEF and LVX interacted physically with CS-AgNPs strongly, replacing the citrate molecules on surface and forming antibiotic-CS-AgNPs complexes.[26] Moreover, these antibiotics readily caused aggregation of CS-AgNPs at higher concentrations, while no such aggregation was observed for AMX. However, the molecular nature of the interaction between the CS-AgNPs and the different antibiotics needs further investigation.

## Antibacterial Activity of AgNPs, CS-AgNPs and Antibiotic-Loaded CS-AgNPs

The antibacterial activity of SAEE, CS, AgNPs, CS-AgNPs, and antibiotics-loaded CS-AgNPs were evaluated against five clinical pathogens using the Oxford cup diffusion method. Table 1 and Figures 1–3 show the zone of inhibitions produced by tested antibacterial solutions against the selected clinical isolates. Amongst all pathogenic strains, CS-AgNPs exhibited a maximum antibacterial effect against *Pseudomonas aeruginosa* (18.4 ± 0.30 mm), and its conjugation with LVX, produced more augmented response (32.5 ± 2.60 mm). A similar trend was observed with other antibiotics-conjugated with CS-AgNPs. The antibacterial mechanism of metal NPs is still not identified, but few studies have reported the plausible

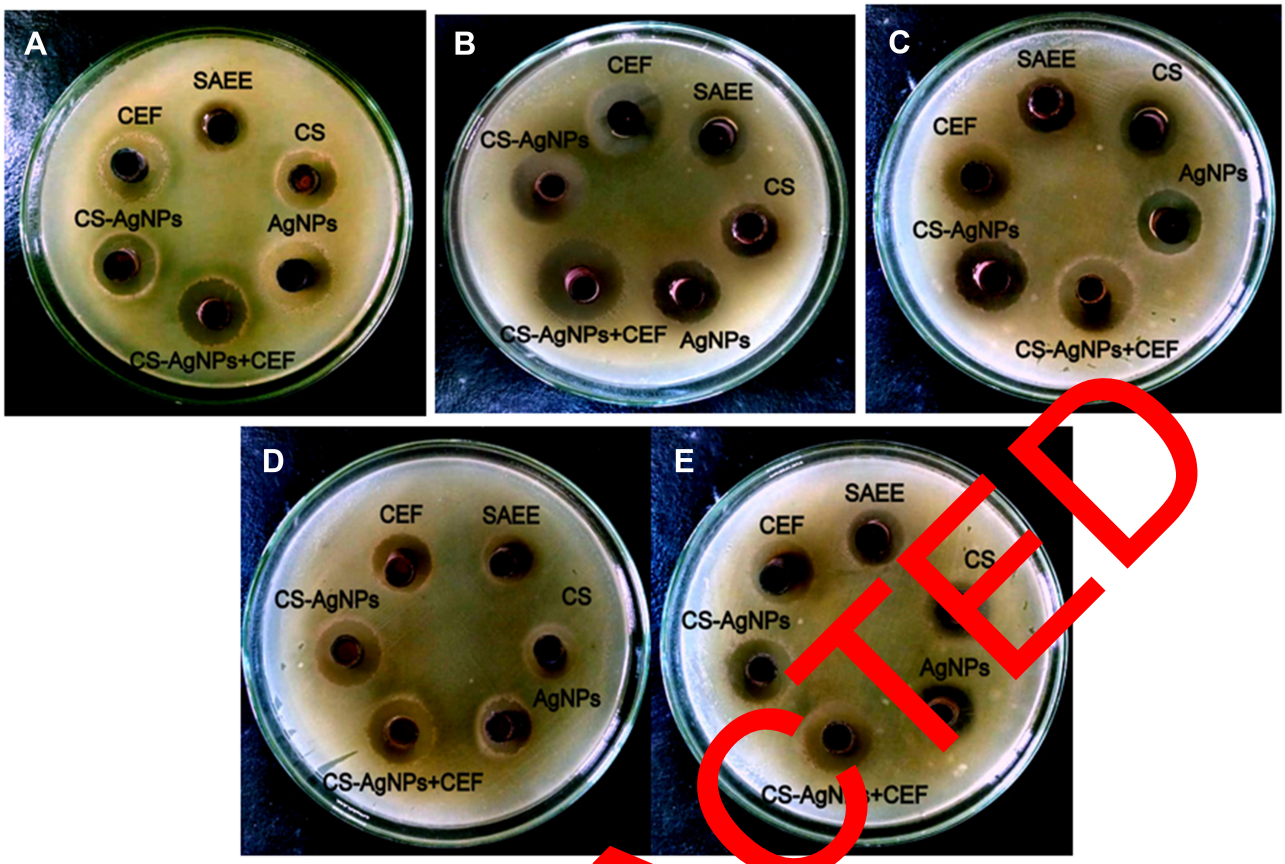




**Figure 2** Antibacterial activities of CS-AgNP with cefixime against (**A**) *Escherichia coli*; (**B**) *Klebsiella pneumoniae*; (**C**) *Staphylococcus aureus*; (**D**) *Salmonella typhi*; (**E**) *Pseudomonas aeruginosa*.

mechanism like Reidy et al (2013) have suggested that metal NPs have more significant antibacterial effects due to their high affinity with the surface-active groups of microbial strains.[47] Wypij et al (2018) and Rai et al (2012) have reported that the released metal ions from NPs can rapture the bacterial cell wall and can cause cell death.[21,48] Moreover, the distortion of bacterial DNA helical structure by a metal ion has also been reported.[49,50] In addition, chitosan has been suggested to react with both the bacterial cell wall and the cell membrane.[51]

All the antibiotics combined with CS-AgNPs showed enhanced antibacterial potential against all tested pathogens ($p \leq 0.003$). The fold increase in zones is reflected in Figure 4. Interestingly, antibiotics like AMX and CEF showed minimal susceptibility, when conjugated with CS-AgNPs exhibited potential antibacterial activity against *Klebsiella pneumoniae* and *Staphylococcus aureus* respectively after conjugation as reflected in Table 1. CEF showed the highest fold increase in its activity against *Staphylococcus aureus* (1.8) while AMX and LVX showed 2.2 and 1.2 fold increase in their activity, respectively, against *Klebsiella pneumoniae* when conjugated with CS-AgNPs. Different researchers have also been reported the synergistic activity of antibiotics when they were combined with AgNPs, synthesized by different methods.[18,22,52]

CS-AgNPs exhibited low values of MICs against all tested isolates (32 µg/mL) compared to AgNPs (64 µg/mL) as presented in Table 2. The results of MIC assays after conjugation are given in Table 3. The MICs of all antibiotics reduced considerably when combined with CS-AgNPs against all pathogenic strains, and maximum reduction in MIC was observed for AMX from 1024 to 64 and 32 µg/mL against *Escherichia coli* and *Klebsiella pneumoniae*, respectively. The FIC values ranging from 0.12 to 0.25 for all antibiotics conjugations against the tested isolates demonstrated their synergistic activity (Table 3). The previous study reported the comparable synergistic response of synthesized AgNPs with different antibiotics.[21] In the present work, the MBC value of CS-AgNPs was found to be 32 µg/mL against all tested isolates (Table 4). However, these values reduced drastically after conjugation with different antibiotics ranging from 32 to 4 µg/mL.

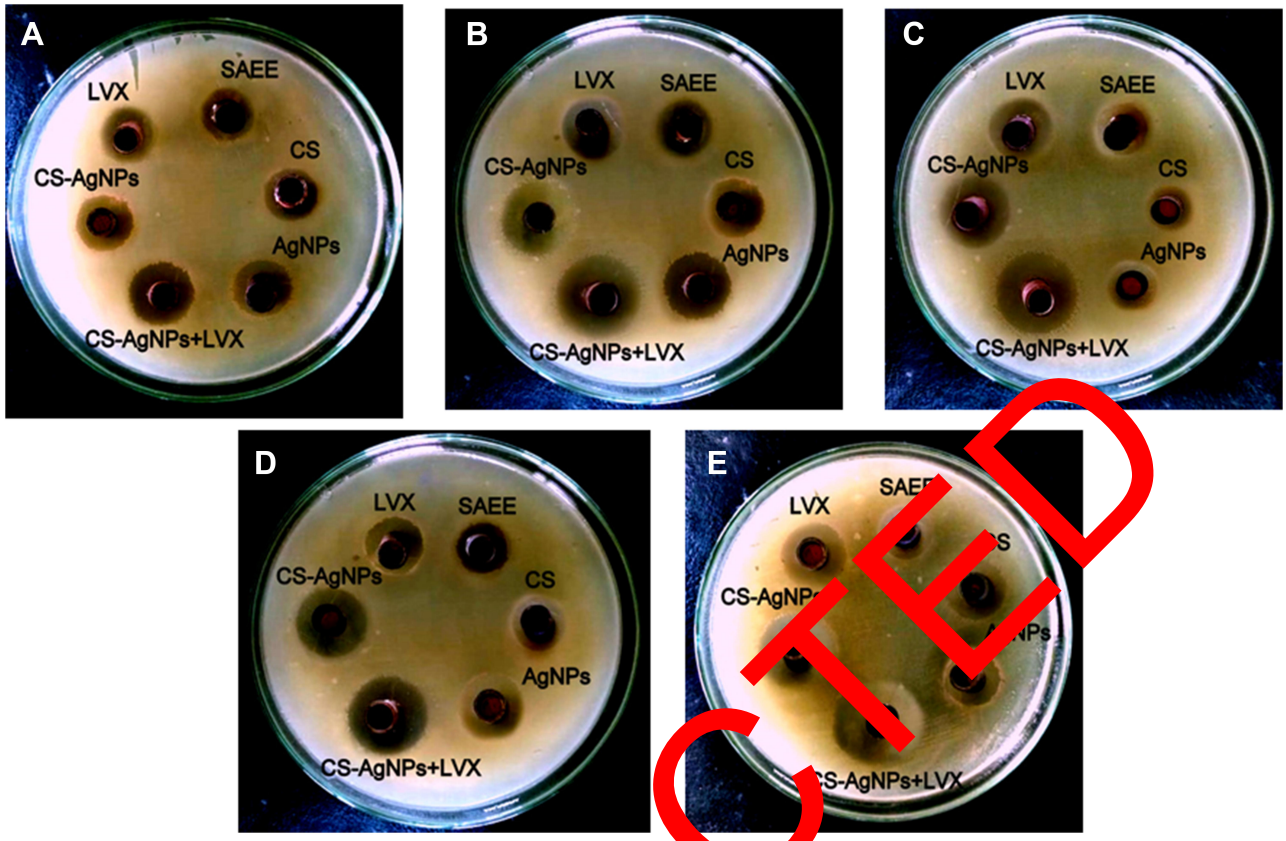


**Figure 3** Antibacterial activities of CS-AgNP with levofloxacin against (**A**) *Escherichia coli*; (**B**) *Klebsiella pneumoniae*; (**C**) *Staphylococcus aureus*; (**D**) *Salmonella typhi*; (**E**) *Pseudomonas aeruginosa*.

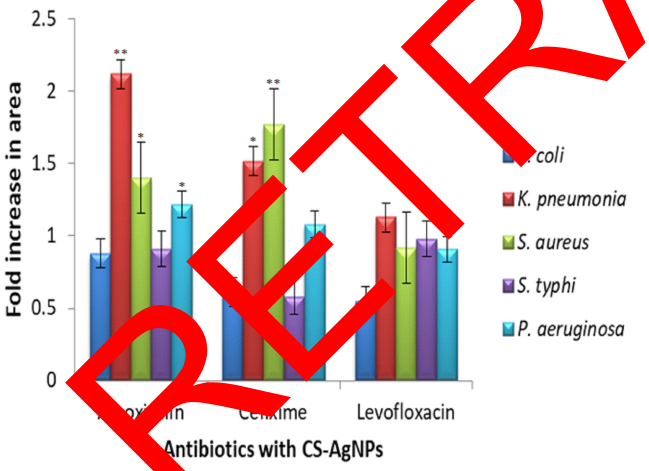


**Figure 4** Fold increase in inhibition zones of antibiotics after conjugation with CS-AgNPs against tested isolates. All experiments were performed in triplicates and reported as mean ± SD. *$p \leq 0.05$ significant as compared to control (considered as no increase in activity), **$p \leq 0.005$ highly significant as compared to control.

## Mechanism of Synergistic Effects

Silver nanoparticles (AgNPs) exhibit very distinctive physicochemical characteristics, and tremendous antibacterial activity, which highly recommend them as an alternative treatment against multi-drug resistant bacteria.[53,54] Biogenic silver nanoparticles reported showing greater antibiofilm activity against these superbugs.[55] Nanocomposites of silver with other metals observed the disruption of biofilm structure and penetration of metal ions into under layers of bacterial colony.[56] Chitosan conjugated nanocomposites have profound antibacterial activity, due to the presence of an ammonia group in chitosan. Ammonia adsorbs on to the cell wall electrostatically and potentiates the destruction of cell wall by causing leaking of macromolecules from the bacterial cell.[12,57] It is reported that synergistic antibacterial activity of chitosan with AgNPs may be resulted due to blistering (blebs), blockage of the electron transport chain, and clumping of membranes.[54] In addition, chemical interaction as the possible cause of the synergistic rise in antibacterial activity of the synthesized AgNPs with antibiotic.[31,58] However, it was also postulated that the combined effect of antimicrobials drives synergy by membrane alterations generated by AgNPs, and no chemical interactions were detected between AgNPs and antibiotics.[59] Moreover, it was also reported that amino and hydroxyl groups present in tested

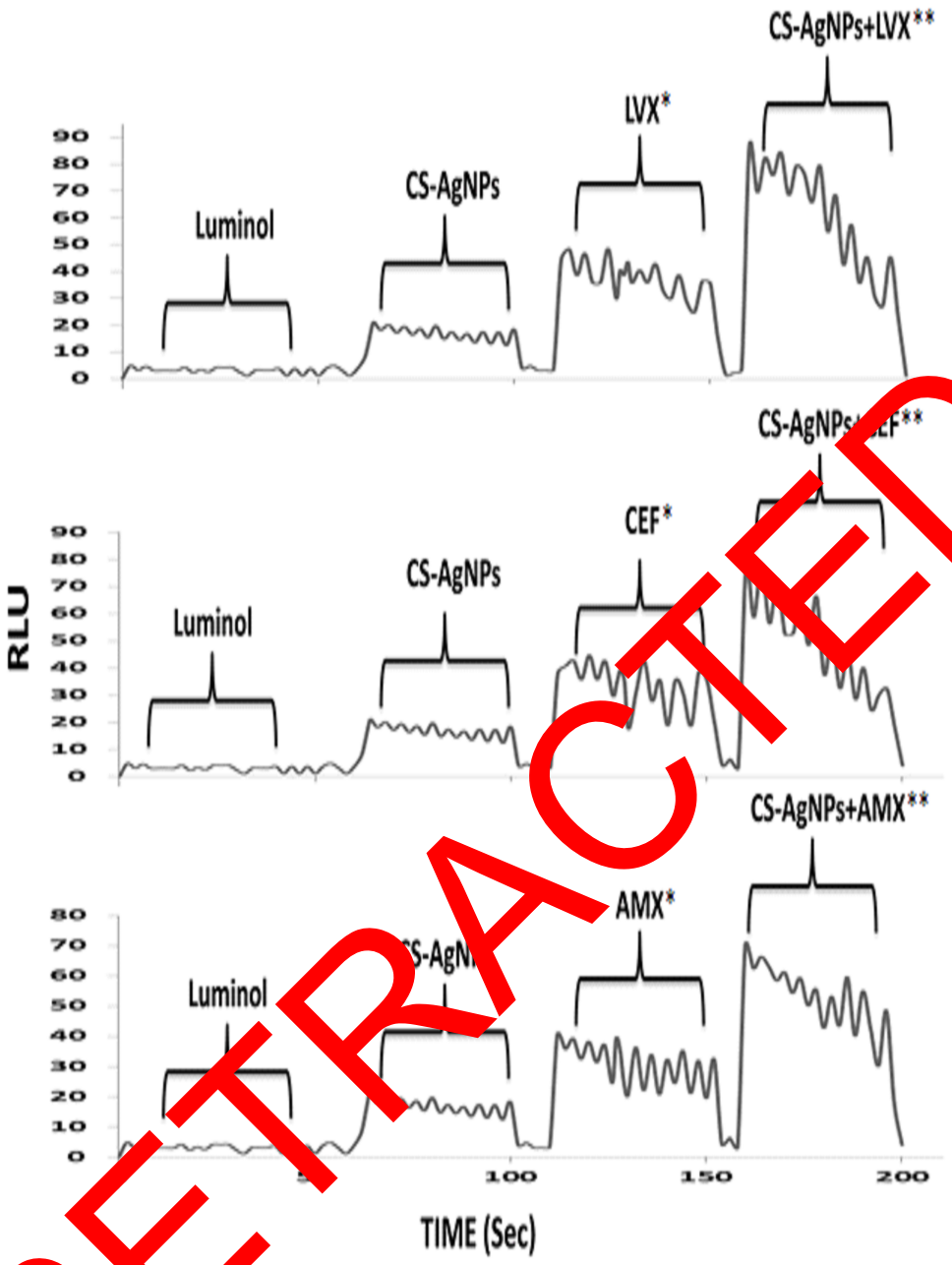


**Figure 5** CS-AgNPs associated generation of hydroxyl radicals in the presence of different antibacterial agent. *The chemiluminescence of luminol (stage 1) in the presence of CS-AgNPs (stage 2) antibiotics (stage 3) CS-AgNPs combined with different antibiotics (stage 4). **RLU, relative luminescence units; AMX, amoxicillin; CEF, cefixime; LVX, levofloxacin. All experiments were performed in triplicates and reported as mean. *$p \leq 0.05$ significant as compared to control (luminol), **$p \leq 0.005$ highly significant as compared to control.



antibiotics bind with CS-AgNPs by chelation, which may maximize agglomeration and increase antibacterial activity.[19] Kohanski et al (2007) suggested that production of hydroxyl radicals is an intriguing bacterial killing mechanism of several antibiotics.[60] Consistent with reported studies, we tested whether or not bacterial cells treated with AgNPs generated hydroxyl radicals and how this affected the synergistic effects. In the luminol model, synthesized CS-AgNPs generated hydroxyl radicals as shown in Figure 5. All studied bactericidal antibiotics, caused the formation of hydroxyl radicals. However, treatment with combinations of CS-AgNPs and antibiotics showed increased hydroxyl radical formation compared with each antibacterial agent alone. Results indicated a significant increase in the generation of hydroxyl radicals, which might be an important cause

**Table 2** Minimum Inhibitory Concentrations (MICs) of Different Antibacterial Agents Against Clinical Isolates

| Antibacterial Agents | Minimum Inhibitory Concentrations (μg/mL) (Mean ± S.D) | | | | |
|---|---|---|---|---|---|
| | *E. coli* | *K. pneumoniae* | *S. aureus* | *S. typhi* | *P. aeruginosa* |
| SAEE | 7500 ± 245.3 | 7500 ± 211.4 | 7500 ± 254.2 | 7500 ± 287.2 | 7500 ± 241.2 |
| CS | 256 ± 14.7 | 256 ± 15.5 | 256 ± 26.3 | 256 ± 17.5 | 256 ± 18.4 |
| AgNPs | 64 ± 9.4 | 64 ± 14.5 | 64 ± 8.4 | 64 ± 5.1 | 64 ± 9.3 |
| CS-AgNPs | 32 ± 3.4 | 32 ± 11.4 | 32 ± 6.5 | 32 ± 4.1 | 32 ± 7.3 |
| AMX | 1024 ± 141.2 | 1024 ± 102.4 | 256 ± 22.5 | 256 ± 29.4 | 512 ± 64.7 |
| CEF | 256 ± 12.4 | 128 ± 26.4 | 256 ± 22.4 | 32 ± 3.0 | 256 ± 23.4 |
| LVX | 16 ± 2.3 | 64 ± 7.9 | 128 ± 24.8 | 1 ± 0.12 | 1024 ± 126.4 |

**Note:** All experiments were performed in triplicates and reported as mean ± SD.
**Abbreviations:** S.D, standard deviation; SAEE, *Syzygium aromaticum* ethanolic extract; CS, chitosan; AMX, amoxicillin; CEF, cefixime; LVX, levofloxacin.

**Table 3** Fractional Inhibitory Concentration (FIC) Index and Minimum Inhibitory Concentrations (MICs) of Antibiotics-Conjugated CS-AgNPs Against Clinical Isolates

| Clinical Isolates | Fractional Inhibitory Concentration (FIC) Index | | | | | |
|---|---|---|---|---|---|---|
| | CS-AgNPs + AMX | | CS-AgNPs + CEF | | CS-AgNPs + LVX | |
| | FIC | MIC of CS-AgNPs + AMX | FIC | MIC of CS-AgNPs + CEF | FIC | MIC of CS-AgNPs + LVX |
| *E. coli* | 0.12 | 4 + 64 | 0.18 | [illegible] + 32 | 0.12 | 4 + 1 |
| *K. pneumoniae* | 0.15 | 8 + 32 | 0.12 | [illegible] + 8 | 0.18 | 8 + 4 |
| *S. aureus* | 0.18 | 4 + 16 | 0.18 | [illegible] + 16 | 0.15 | 4 + 4 |
| *S. typhi* | 0.18 | 4 + 16 | 0.18 | 4 + [illegible] | 0.12 | 2 + 0.0625 |
| *P. aeruginosa* | 0.18 | 4 + 32 | [illegible] | 4 + 32 | 0.25 | 4 + 128 |

**Abbreviations:** AMX, amoxicillin; CEF, cefixime; LVX, levofloxacin.

**Table 4** Biocompatibility Index (BI) and Minimum Bactericidal Concentration (MBC) Values of Antibiotics of Different Antibacterial Agents Against Clinical Isolates

| Antibacterial Agents | Biocompatibility Index (BI) | | | | | | | | | | |
|---|---|---|---|---|---|---|---|---|---|---|---|
| | *E. coli* | | *K. pneumoniae* | | *S. aureus* | | *S. typhi* | | *P. aeruginosa* | | $IC_{50}$ (μg/mL) |
| | BI | MBC | BI | MBC | BI | MBC | BI | MBC | BI | MBC | |
| AgNPs | 1.6 | 64 | 1.6 | 64 | 1.6 | 64 | 1.6 | 32 | 1.6 | 64 | 102.7* |
| CS-AgNPs | [illegible] | 32 | 3.9 | 32 | 3.9 | 32 | 3.9 | 32 | 3.9 | 32 | 125.7* |
| AMX | [illegible] | [illegible]024 | 0.1 | 1024 | 0.7 | 256 | 0.3 | 512 | 0.1 | 1024 | 194.6 |
| CS-AgNPs + AMX | 5.2+[illegible] | 16+64 | 5.2+1.4 | 16+128 | 5.2+1.4 | 16+128 | 10.4+2.8 | 8+64 | 5.2+2.8 | 16+64 | 84.4+180.1 |
| CEF | [illegible] | 512 | 0.7 | 256 | 0.3 | 512 | 2.8 | 64 | 0.3 | 512 | 179.3 |
| CS-AgNPs + CEF | 4.9+2.4 | 16+64 | 4.9+9.9 | 16+16 | 4.9+2.4 | 16+64 | 9.9+39.6 | 8+4 | 4.9+2.4 | 16+64 | 79.8+158.4 |
| LVX | 5.2 | 32 | 1.3 | 128 | 0.6 | 256 | 83.4 | 2 | 0.16 | 1024 | 166.8 |
| CS-AgNPs + LVX | 8.1+37.4 | 8+4 | 2.0+2.3 | 32+64 | 8.1+4.6 | 8+32 | 16.2+149.9 | 4+1 | 4.0+1.1 | 16+128 | 65.0+149.9 |

**Note:** *These $IC_{50}$ values were taken from our previous study [Muhammad Arif et al 2020].
**Abbreviations:** MBC, minimum bactericidal concentration; $IC_{50}$, inhibitory concentration; AMX, amoxicillin; CEF, cefixime; LVX, levofloxacin.

of the synergism seen. It is suggested that oxidative stress caused by AgNPs through increase in radicals production leads to damage of the nucleic acids and proteins, and consequently inhibition of proliferative processes in bacterial cells.[55] Researchers confirmed that AgNPs produced different toxic radicals including hydrogen peroxide ($H_2O_2$) and hydroxyl radicals (OH).[61,62] Moreover, results of physical interaction investigation also pointed out that the bacterial cells were killed more effectively by "CS-AgNPs-antibiotic complexes", which is in consistent

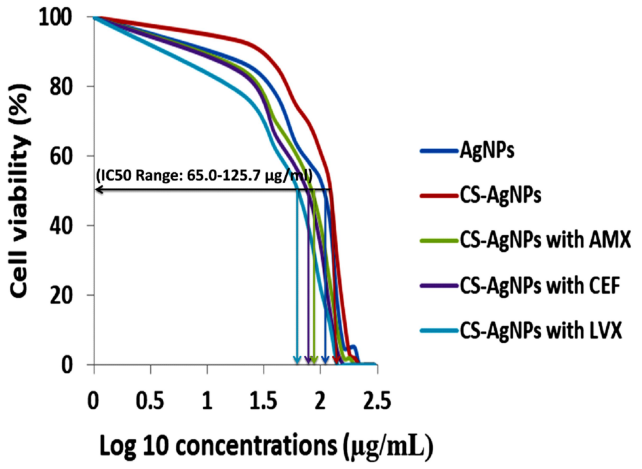


**Figure 6** % viability of HeLa cells against AgNPs, CS-AgNPs alone, and combination with different antibiotics while $IC_{50}$ of each agent are given in Table 4. All experiments were performed in triplicates and reported as mean.

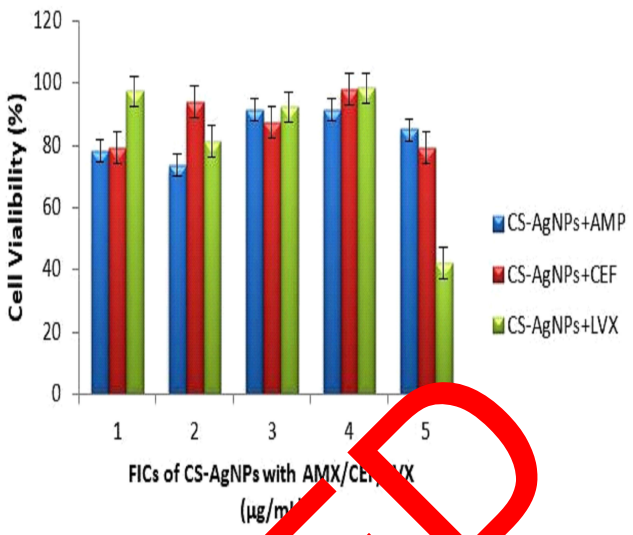


**Figure 7** Cytotoxic activity of combined antibacterial agents (CS-AgNPs and antibiotics) against HeLa cell line. Bacterial microbials were used at concentrations of their FIC. 1 = (4 µg/mL of CS-AgNPs+4 µg/mL AMX or 32 µg/mL CEF or 1 µg/mL LVX); 2 = (8 µg/mL of CS-AgNPs+32 µg/mL AMX or 4 µg/mL of CS-AgNPs+8 µg/mL CEF or 8 µg/mL of CS-AgNPs+4 µg/mL LVX); 3 = (4 µg/mL of CS-AgNPs+16 µg/mL AMX or CEF or 4 µg/mL LVX); 4 = (4 µg/mL of CS-AgNPs+16 µg/mL AMX or 2 µg/mL CEF or 2 µg/mL of CS-AgNPs+0.0625 µg/mL LVX); 5 = (4 µg/mL of CS-AgNPs+128 µg/mL AMX or CEF or 128 µg/mL LVX). AMX, amoxicillin; CEF, cefixime; LVX, levofloxacin.

with previous study.[26] However, the exact molecular mechanism by which increase in production of radical species, still requires further studies.

## Toxicity Studies

### In vitro Cytotoxic Evaluation of Antibiotics-Loaded CS-AgNPs

The antibiotics-loaded CS-AgNPs were subjected to evaluate the cytotoxicity on the HeLa cell lines. The dose-dependent effects of all tested solutions were observed against eukaryotic cells. The $IC_{50}$ values of AMX, CEF and LVX was found to be 194, 17[illegible], and [illegible] µg/mL, respectively (Table 4). The percentage viability of HeLa cells at different concentrations of AgNPs, CS-AgNPs alone and in combination with different antibiotics is also presented in Figure 6. In our previous work, $IC_{50}$ value of CS-AgNPs was reported as 125 µg/mL.[23] In the current study, $IC_{50}$ values of CS-AgNPs were slightly decreased after conjugation with different antibiotics. However, a considerable reduction in MICs and FICs (Tables 2 and 3, Figure 7), suggested the dose reduction

**Table 5** Body Weight and Relative Major Organ Weights of Both Male and Female Rats After 28th Day's Exposure of CS-AgNPs at Different Concentrations

| Groups | Body Weight Gain (Mean ± S.D) (After 28th Days) | Relative Major Organ Weights (% ± S.D) (After 28th Days) | | | | |
|---|---|---|---|---|---|---|
| | | Brain | Heart | Kidneys | Liver | Lungs |
| Male | | | | | | |
| Control | 24.4 ± 4.2 | 0.61 ± 0.04 | 0.36 ± 0.01 | 1.02 ± 0.09 | 4.33 ± 0.23 | 0.47 ± 0.07 |
| CS-AgNPs (30 mg/kg) | 22.8 ± 3.0 | 0.58 ± 0.02 | 0.34 ± 0.03 | 0.98 ± 0.12 | 4.57 ± 0.25 | 0.43 ± 0.09 |
| CS-AgNPs (60 mg/kg) | 19.7 ± 8.1 | 0.60 ± 0.04 | 0.33 ± 0.03 | 0.93 ± 0.06 | 4.66 ± 0.37 | 0.52 ± 0.10 |
| CS-AgNPs (90 mg/kg) | 18.1 ± 7.1 | 0.63 ± 0.01 | 0.35 ± 0.02 | 1.01 ± 0.10 | 4.72 ± 0.20 | 0.45 ± 0.05 |
| Female | | | | | | |
| Control | 18.9 ± 5.7 | 0.53 ± 0.03 | 0.38 ± 0.02 | 1.04 ± 0.05 | 4.12 ± 0.18 | 0.52 ± 0.04 |
| CS-AgNPs (30 mg/kg) | 19.3 ± 5.3 | 0.51 ± 0.05 | 0.36 ± 0.01 | 1.07 ± 0.04 | 4.41 ± 0.13 | 0.48 ± 0.10 |
| CS-AgNPs (60 mg/kg) | 20.4 ± 6.9 | 0.58 ± 0.07 | 0.30 ± 0.04 | 1.02 ± 0.11 | 4.37 ± 0.40 | 0.43 ± 0.02 |
| CS-AgNPs (90 mg/kg) | 19.0 ± 5.4 | 0.55 ± 0.02 | 0.36 ± 0.03 | 0.99 ± 0.07 | 4.48 ± 0.20 | 0.51 ± 0.07 |

**Note:** All experiments were performed in triplicates and reported as percentage ± SD.
**Abbreviation:** S.D, standard deviation (n=10).

**Table 6** Hematological and Biochemical Parameters of Both Male and Female Rats After 28th Day's Exposure of CS-AgNPs at Different Concentrations

| Parameters | Groups* (Mean ± S.D) | | | | | | | |
|---|---|---|---|---|---|---|---|---|
| | Male | | | | Female | | | |
| | Control | CS-AgNPs (30 mg/kg) | CS-AgNPs (60 mg/kg) | CS-AgNPs (90 mg/kg) | Control | CS-AgNPs (30 mg/kg) | CS-AgNPs (60 mg/kg) | CS-AgNPs (90 mg/kg) |
| **Serum electrolytes** | | | | | | | | |
| $Na^+$ (mEq/L) | 135.4 ± [illegible].54 | [illegible]9.2 ± 6.2[illegible] | 134.6 ± 8.46 | 142.2 ± 11.57 | 137.5 ± 6.91 | 134.8 ± 8.43 | 138.7 ± 6.91 | 138.2 ± 7.73 |
| $K^+$ (mEq/L) | 5.64 ± 0.78 | 6.0[illegible] ± 0.61 | 5.89 ± 0.56 | 4.94 ± 1.08 | 5.24 ± 0.59 | 5.83 ± 0.73 | 6.09 ± 0.48 | 5.63 ± 0.77 |
| $Ca^+$ (mEq/L) | 5.28 ± 0.70 | 5.41 ± 0.82 | 5.32 ± 0.48 | 6.08 ± 1.12 | 5.06 ± 0.43 | 5.37 ± 0.60 | 5.57 ± 0.17 | 5.30 ± 0.35 |
| **Blood profile** | | | | | | | | |
| RBCs ($10^{12}$/L) | 8.42 ± 0.63 | 8.17 ± 0.5[illegible] | 8.35 ± [illegible]2 | 8.09 ± 0.72 | 7.97 ± 0.51 | 7.99 ± 0.70 | 7.83 ± 0.62 | 7.70 ± 0.48 |
| WBCs ($10^9$/L) | 13,485 ± 3482 | 14,834 ± [illegible]4870 | 15[illegible]7 ± 7[illegible]4 | 15,873 ± 8340* | 11,540 ± 4017 | 12,604 ± 5137 | 13,034 ± 5379 | 13,974 ± 7842* |
| Basophils (%) | 0.00 ± 0.00 | 0.00 ± 0.00 | [illegible] ± 0.00 | 0.60 ± 0.04* | 0.00 ± 0.00 | 0.00 ± 0.00 | 0.00 ± 0.00 | 0.60 ± 0.06* |
| Eosinophils (%) | 1.87 ± 0.20 | 1.44 ± 0.17 | 1.72 ± [illegible]21 | 2.87 ± 0.38* | 2.49 ± 0.14 | 1.72 ± 0.28 | 2.92 ± 0.36 | 3.47 ± 0.24* |
| Lymphocytes (%) | 75.89 ± 6.87 | 78.07 ± 8.16 | 81.56 ± [illegible]11.36 | 89.94 ± 12.57* | 78.15 ± 7.46 | 80.17 ± 5.42 | 79.05 ± 8.47 | 91.53 ± 9.91* |
| Monocytes (%) | 1.45 ± 0.27 | 1.48 ± 0.14 | 1.51 ± [illegible]0.23 | [illegible] ± 0.68 | 1.37 ± 0.34 | 1.53 ± 0.39 | 1.46 ± 0.16 | 2.59 ± 0.41 |
| Neutrophils (%) | 22.41 ± 5.98 | 24.73 ± 4.21 | 29.4[illegible] ± 5.0[illegible] | 34.[illegible]9 ± 9.40* | 19.86 ± 4.76 | 22.33 ± 5.91 | 26.74 ± 4.37 | 37.08 ± 5.10* |
| Hb levels (g/dL) | 14.98 ± 0.94 | 14.56 ± 0.85 | 15.20 ± [illegible].98 | [illegible]12 ± 1.12 | 13.47 ± 0.57 | 13.82 ± 0.97 | 13.27 ± 0.62 | 14.01 ± 0.83 |
| ESR (mm/h) | 1.42 ± 0.27 | 1.48 ± 0.43 | 1.43 ± 0.69 | [illegible].54 ± 0[illegible] | 1.53 ± 0.18 | 1.46 ± 0.37 | 1.53 ± 0.56 | 1.58 ± 0.39 |
| **Liver profile** | | | | | | | | |
| ALP (U/L) | 218.47 ± 28.7 | 285.41 ± 87.6 | 312.56 ± 74.0* | 44[illegible]98 ± 102.5** | 2[illegible]60 ± 25.3 | 267.38 ± 69.3 | 298.19 ± 37.6 | 430.41 ± 58.3** |
| AST (U/L) | 235.72 ± 39.4 | 312.40 ± 28.1 | 378.37 ± 56.8* | 439.[illegible] ± 67.5** | 203.4[illegible] ± 24.3 | 240.37 ± 37.6 | 311.98 ± 34.2* | 381.09 ± 43.1** |
| ALT (U/L) | 43.21 ± 18.27 | 59.79 ± 14.08 | 62.13 ± 17.25* | 81.19 ± [illegible]* | 52.[illegible] ± [illegible]31 | 61.08 ± 12.40 | 68.97 ± 20.73* | 75.37 ± 19.33** |
| Bilirubin (mg/dL) | 0.68 ± 0.14 | 0.52 ± 0.17 | 0.81 ± 0.13* | 0.99 ± 0.10** | [illegible]6 ± 0.24 | 0.64 ± 0.42 | 0.73 ± 0.37* | 0.92 ± 0.29** |
| **Kidney profile** | | | | | | | | |
| Creatinine (mg/dL) | 1.87 ± 0.24 | 1.82 ± 0.14 | 1.85 ± 0.21 | 1.86 ± 0.17 | 1.13 ± [illegible] | [illegible]0 ± 0.24 | 1.21 ± 0.11 | 1.18 ± 0.29 |
| BUN (mg/dL) | 28.70 ± 2.41 | 27.21 ± 3.87 | 29.05 ± 3.28 | 25.96 ± 4.84 | 26.2[illegible] ± 3.19 | 26.97 ± 2.72 | 28.33 ± 3.94 | 27.94 ± 3.48 |
| Uric acid (mg/dL) | 1.71 ± 0.14 | 1.68 ± 0.08 | 1.73 ± 0.10 | 1.74 ± 0.19 | 1.67 ± [illegible]0.18 | 1.70 ± [illegible] | 1.68 ± 0.32 | 1.66 ± 0.24 |
| **Cardiac Profile** | | | | | | | | |
| CK-MB (IU/mL) | 12.84 ± 0.26 | 12.06 ± 0.19 | 11.97 ± 0.51 | 12.15 ± 0.18 | 13.10 ± 0.62 | 12.42 ± 0.36 | 13.18 ± 0.47 | 12.52 ± 0.29 |
| Cholesterol (mg/dL) | 72.84 ± 12.74 | 71.68 ± 14.87 | 72.62 ± 13.87 | 70.02 ± 17.45 | 77.67 ± 10.67 | 79.34 ± 12.1[illegible] | 78.04 ± 14.93 | 78.90 ± 9.82 |
| **Inflammatory biomarkers** | | | | | | | | |
| CRP (mg/dL) | 60.45 ± 4.58 | 66.91 ± 7.48 | 69.73 ± 5.81 | 86.13 ± 7.34* | 57.33 ± 5.39 | 60.90 ± 6.53 | 64.74 ± 5.52 | 83.62 ± 7.67* |
| IL-1 (pg/mL) | 38.78 ± 3.34 | 41.37 ± 4.67 | 46.85 ± 4.65 | 59.62 ± 5.32 | 37.99 ± 4.25 | 43.75 ± 4.76 | 48.92 ± 6.78 | 57.67 ± 4.34* |
| IL-2 (pg/mL) | 22.14 ± 3.45 | 26.22 ± 4.87 | 31.58 ± 5.82 | 39.32 ± 3.66* | 26.85 ± 5.24 | 31.48 ± 4.10 | 35.34 ± 6.08 | 45.08 ± 6.84* |

(*Continued*)

**Table 6** (Continued).

| Parameters | Groups* (Mean ± S.D) | | | | | | | |
|---|---|---|---|---|---|---|---|---|
| | Male | | | | Female | | | |
| | Control | CS-AgNPs (30 mg/kg) | CS-AgNPs (60 mg/kg) | CS-AgNPs (90 mg/kg) | Control | CS-AgNPs (30 mg/kg) | CS-AgNPs (60 mg/kg) | CS-AgNPs (90 mg/kg) |
| IL-6 (pg/mL) | 59.44 ± 4.3[illegible] | 61.[illegible] ± 5.98 | 63.89 ± 5.56 | 89.97 ± 10.85* | 58.54 ± 4.30 | 63.79 ± 6.53 | 69.12 ± 7.93 | 87.85 ± 9.01* |
| IL-10 (pg/mL) | 10.26 ± 3.21 | 12.68 ± 3.53 | [illegible]5.85 ± 4.36 | 23.53 ± 3.54* | 13.27 ± 4.34 | 16.56 ± 3.62 | 19.95 ± 3.27 | 27.62 ± 5.95* |
| TNF-α (pg/mL) | 17.85 ± 2.78 | [illegible]9.45 ± 3.67 | 22.[illegible] ± 4.81 | 34.95 ± 4.10 | 18.03 ± 2.87 | 21.98 ± 4.86 | 25.16 ± 4.88 | 33.68 ± 5.87* |

**Notes:** All experiments were performed in triplicates and reported as mean ± S.D. (n=10), *p ≤ 0.05 significant as compared to control, **p ≤ 0.005 highly significant as compared to control.
**Abbreviations:** S.D, standard deviation; RBCs, red blood cells; WBCs, white blood cells; Hb, hemoglobin; ESR, erythrocyte sedimentation rate; ALP, alkaline phosphatase; AST, alkaline phosphatase; ALT, alanine transaminase; BUN, blood urea nitrogen; CK-MB, creatine kinase-MB; CRP, C-reactive protein; IL, interleukin; TNF-α, tumor necrotic factor α.

with minimal potential toxicity, which is corresponded with a previous study.[21] Researchers claimed that the combination of antibiotics with silver nanoparticles restored the antibacterial potential of these agents against resistance acquired bacteria along with the reduction in toxicity.[18,22] These observations are also in agreement with the present study, where the BI values after conjugation with antibiotics were found more than 1, expressing more bactericidal activity with low toxicity (Table 4).

## In vivo Acute and Sub-Acute Toxicity Studies of CS-AgNPs

Initially, the acute oral toxicity of synthesized CS-AgNPs was determined for 14 days. No significant sign of toxicity was observed in studied animals after 14 days of oral dosing of CS-AgNPs. The $LD_{50}$ value of CS-AgNPs was found to be >200 mg/kg, resembled previous findings.[63] In the sub-acute study, no significant changes were observed at any dose of CS-AgNPs in both male and female body weights and relative organ weights compared to control groups (P<0.05) Table 5. All studied groups animals survived until the euthanasia was performed for further studies. Furthermore, no sign of adverse effects or any infection noticed during the study period of 28 days. Lee et al also reported similar observations after the treatment of rats with AgNPs at concentrations of 500 mg/kg.[37]

In the present work, the effect of gender was not observed in the hematological and biochemical analysis of Sprague Dawley rats. At the dose of 90 mg/kg, synthesized CS-AgNPs significantly increased the counts of WBCs, basophils, eosinophils, lymphocytes, and neutrophils compared to control at the significance level of P<0.05 (Table 6). There were no significant changes observed in other hematological parameters of studied groups after 28 days of oral dosing. Moreover, serum levels of sodium, potassium, and calcium were found in normal ranges during sub-acute toxicity studies compared to the control group.

The serum biochemical analyses are a widely used tool to assess responses in animals induced by different exogenous chemicals and toxins. These biochemical tests are also used to diagnose various diseases of the liver, kidney, heart, and other organs. The elevated levels of any serum biochemical parameter demonstrate any damaged or dysfunction of organs. After 28 days exposure of CS-AgNPs, significant (P<0.05) and highly significant (P<0.005) increased were observed in alkaline phosphatase (ALP), aspartate transaminase (AST), alanine transaminase

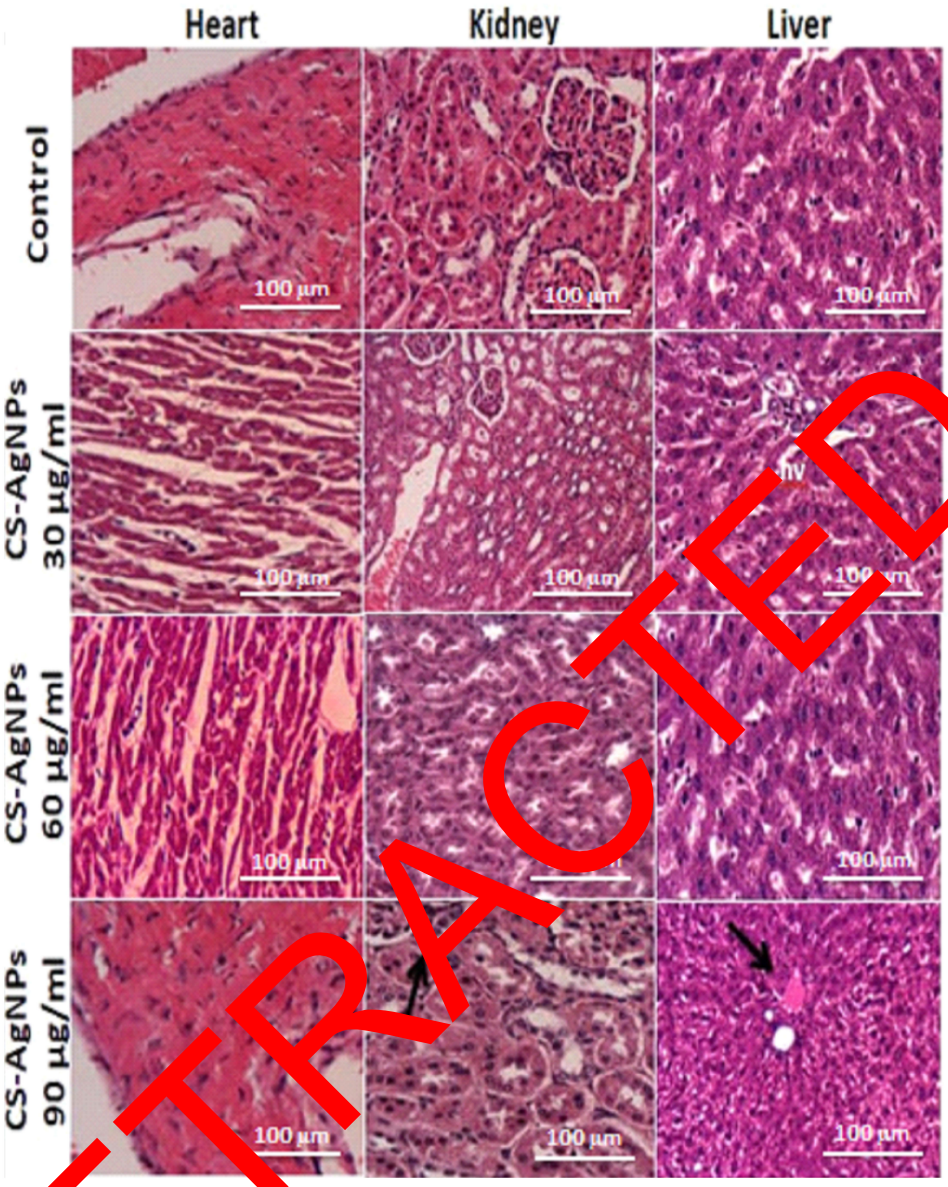




**Figure 8** Histopathological examinations of heart, kidney and liver of male rats after administration of CS-AgNPs at different doses using the 400× magnification. Arrows in figures shows the minor tissue inflammation at higher doses of CS-AgNPs.

(ALT) and bilirubin levels, at the doses of 60 mg/kg and 90 mg/kg respectively. More than 50% increase in bilirubin levels can be demonstrated to hepatocellular injury.[64] The highly significant increase in bilirubin levels at higher doses, implying that liver injury may have occurred. Increased levels of ALP, AST, and ALT also endorsed the possibility of hepatocellular injury. These enzymatic elevations, coupled with hyperbilirubinemia, may also be observed in cholestatic drug reactions.[65] This implies that orally administered CS-AgNPs at higher doses may cause hepatocellular toxic reactions similar to those caused by other drugs. The significant increase in levels of CRP, IL-1, IL-2, IL-6, IL-10 and TNF-α at high doses also indicated the minor tissue inflammation in treated rats. The present observations are also consistent with previously reported results related to the sub-acute oral toxicity of AgNPs.[37,63] In contrast, the normal levels of creatinine, blood urea nitrogen (BUN), uric acid, creatinine kinase (CK-MB), and cholesterol at all doses indicated that CS-AgNPs did not produce any toxic effects on renal and cardiac systems.

Histopathological examinations were performed to evaluate the effects of CS-AgNPs on body organs of male and female rats, ie, heart, kidney, and liver (Figures

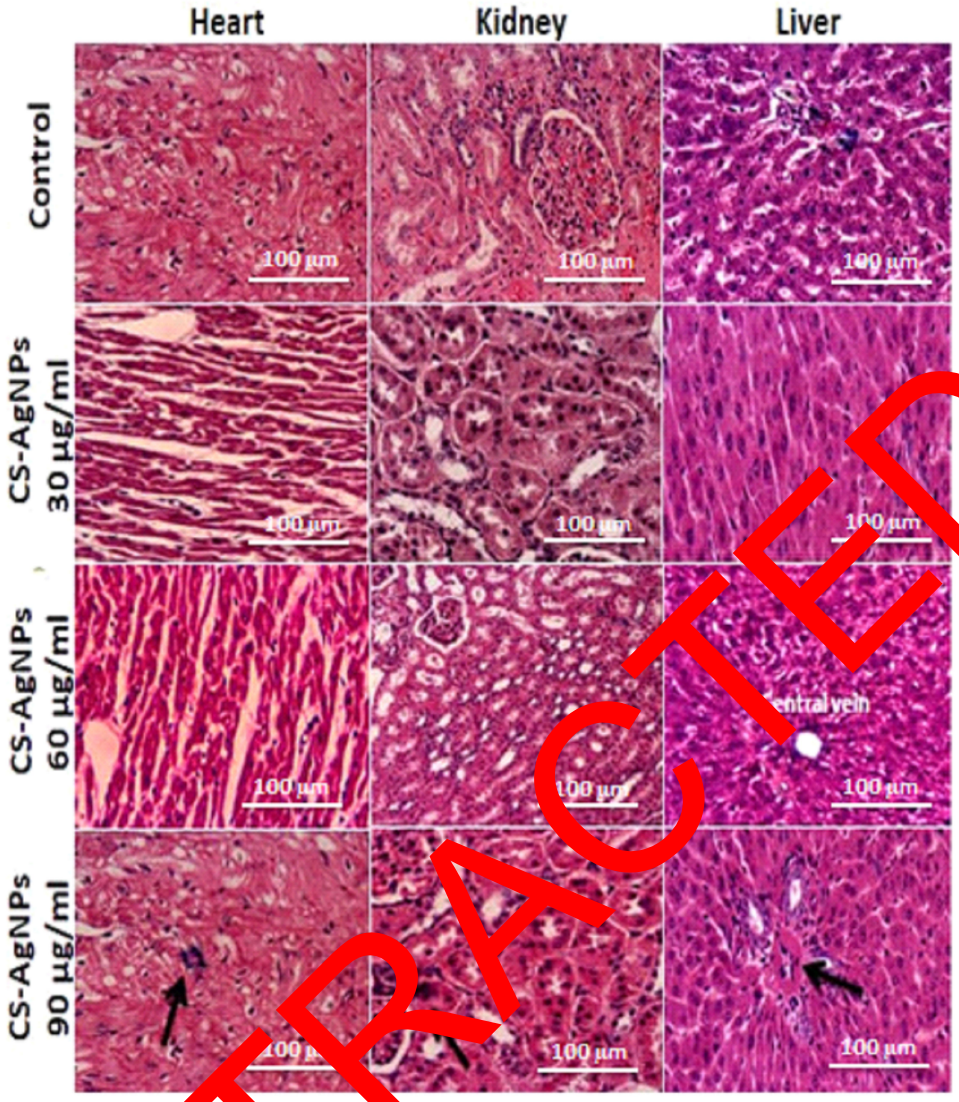


**Figure 9** Histopathological examinations of heart, kidney and liver of female rats after administration of CS-AgNPs at different doses using the 400× magnification. Arrows in figures shows the minor tissue inflammation at higher doses of CS-AgNPs.

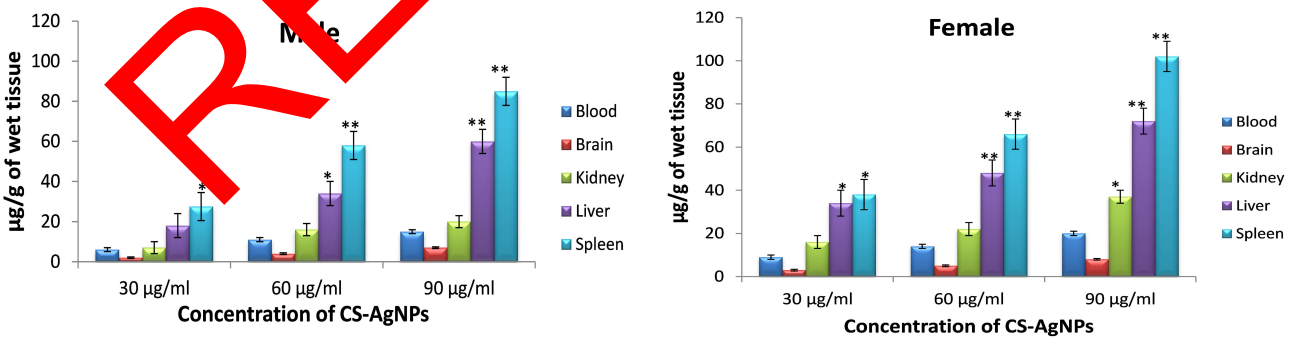


**Figure 10** Silver concentrations (ng/g tissue wet weight) in different organs of both male and female after administration of CS-AgNPs. All experiments were performed in triplicates and reported as mean. *$p \leq 0.05$ significant as compared to control (considered as zero concentration of silver ion), **$p \leq 0.005$ highly significant as compared to control.

8 and 9). Only mild histopathological changes, including inflammation and interstitial hyperemia, were observed only at high dose (90 mg/kg) in the heart, kidney, and liver when exposed to CS-AgNPs, compared to control in both gender groups. Moreover, there were no abnormal changes found at low (30 mg/kg) and medium (60 mg/kg) doses of CS-AgNPs in studied organs. Different researchers also reported the relevant histopathological examinations of AgNPs on different organs and animals at numerous dosing scheduled.[34,63]

## Determination of Silver Ions in Tissues

The concentrations of Ag ion in blood, brain, kidney, liver, and spleen were determined by atomic absorption techniques following the oral administration of CS-AgNPs in rats at the above-defined three doses for 28 days. The concentrations of Ag ion compared to males with female rats at different concentrations of CS-AgNPs are presented in Figure 10. After CS-AgNPs administration, the Ag ion concentrations were highest in the spleen followed by liver, kidney, blood, and brain at all doses in both males and females. At 90 mg/kg, the average levels of Ag ion in the spleen of male and female after 28 days were 85.2 ± 7.8 μg/g and 102.5 ± 9.3 μg/g, respectively, revealing gender difference. These findings are in agreement with previous studies on AgNPs distribution to various tissues at different concentrations.[37,63] Moreover, all organs showed a gender-dependent concentration of Ag ion, with significantly high levels in female compared to male rats following the 28 days administration of all three doses of CS-AgNPs. Kim et al (2008) reported two folds higher accumulation of Ag ion in female compared to male rats.[66] Different researchers also reported similar findings while evaluated the tissue distribution of Ag ion given by different routes, which is suggested that tissue distribution of Ag ion was independent of the administration route.[63,67] Further studies related to the specific mechanisms of the gender-related difference in the distribution of in vivo CS-AgNPs are warranted.

## Conclusion

In the present study, the green synthesized and characterized CS-AgNPs were conjugated and physically interacted with different antibiotics by the simple centrifugation method. The stable functionalization of antibiotics on CS-AgNPs surfaces converses the resistance and increased antibacterial potential many folds against tested pathogenic isolates by radical scavenging potential. Combined therapy also decreases the therapeutic concentration and toxicity. In vivo toxicity studies in rats also confirmed the low toxicity of synthesized CS-AgNPs at a higher dose. Moreover, gender-related differences are found in tissue distribution of Ag ion that is an extensive distribution to the spleen and liver following oral administration. This particular study has pointed out that antibiotic resistance in clinical isolates can be reduced if combined with chitosan functionalized green synthesized silver nanoparticles.

## Acknowledgments

The authors desire to show their gratitude to the Department of Pharmaceutics, Faculty of Pharmacy and Pharmaceutical Sciences, the University of Karachi, for laboratory facilities to conduct this study. The authors also thank the Researchers Supporting Project number (RSP-2020/169), King Saud University, Riyadh, Saudi Arabia.

## Disclosure

The authors report no conflicts of interest in this work.

## References

1. Kumari P, Goswami R, Nimesh S. Application of nanotechnology in diagnosis and therapeutics. *Nanotechnol Energy Environ Eng*. 2020;413–440.
2. Asghar MA, Asghar MA. Green synthesized and characterized copper nanoparticles using various new plants extracts aggravate microbial cell membrane damage after interaction with lipopolysaccharide. *Int J Biol Macromol*. 2020;160:1168–1176. doi:10.1016/j.ijbiomac.2020.05.198
3. Massironi A, Morelli A, Grassi L, et al. Ulvan as novel reducing and stabilizing agent from renewable algal biomass: application to green synthesis of silver nanoparticles. *Carbohydr Polym*. 2019;203:310–321. doi:10.1016/j.carbpol.2018.09.066
4. Asghar MA, Zahir E, Asghar MA, Iqbal J, Rehman AA. Facile, one-pot biosynthesis and characterization of iron, copper and silver nanoparticles using Syzygium cumini leaf extract: as an effective antimicrobial and aflatoxin B1 adsorption agents. *PLoS One*. 2020;15(7):p. e0234964. doi:10.1371/journal.pone.0234964
5. Alavi M, Naser K, Tahereh V. Antibacterial, antibiofilm, antiquorum sensing, antimotility, and antioxidant activities of green fabricated Ag, Cu, TiO2, ZnO, and Fe3O4 NPs via protoparmeliopsis muralis lichen aqueous extract against multi-drug-resistant bacteria. *ACS Biomat Sci Eng*. 2019;5:4228–4243. doi:10.1021/acsbiomaterials.9b00274
6. Vijayakumar V, Samal SK, Mohanty S, Nayak SK. Recent advancements in biopolymer and metal nanoparticle-based materials in diabetic wound healing management. *Int J Biol Macromol*. 2019;122:137–148. doi:10.1016/j.ijbiomac.2018.10.120
7. Tiwari S, Bahadur P. Modified hyaluronic acid based materials for biomedical applications. *Int J Biol Macromol*. 2019;121:556–571. doi:10.1016/j.ijbiomac.2018.10.049
8. Shukla SK, Mishra AK, Arotiba OA, Mamba BB. Chitosan-based nanomaterials: A state-of-the-art review. *Int J Biol Macromol*. 2013;59:46–58. doi:10.1016/j.ijbiomac.2013.04.043
9. Ali A, Ahmed S. A review on chitosan and its nanocomposites in drug delivery. *Int J Biol Macromol*. 2018;109:273–286. doi:10.1016/j.ijbiomac.2017.12.078

10. Morsi RE, Alsabagh AM, Nasr SA, Zaki MM. Multifunctional nanocomposites of chitosan, silver nanoparticles, copper nanoparticles and carbon nanotubes for water treatment: antimicrobial characteristics. *Int J Biol Macromol*. 2017;97:264–269. doi:10.1016/j.ijbiomac.2017.01.032
11. Khawaja H, Zahir E, Asghar MA, Asghar MA. Graphene oxide, chitosan and silver nanocomposite as a highly effective antibacterial agent against pathogenic strains. *Colloid Surface A*. 2018;555:246–255. doi:10.1016/j.colsurfa.2018.06.052
12. Alavi M. Applications of chitosan and nanochitosan in formulation of novel antibacterial and wound healing agents. *In Nanotech in Skin, Soft Tis Bone Infect*. 2020;pp. 169–181.
13. Wei D, Sun W, Qian W, Ye Y, Ma X. The synthesis of chitosan-based silver nanoparticles and their antibacterial activity. *Carbohydr Res*. 2009;344(17):2375–2382.
14. Organization WH. *Antimicrobial Resistance Global Report on Surveillance: 2014 Summary:*. WHO; 2014:1–257.
15. Aslam B, Wang W, Arshad MI, et al. Antibiotic resistance: a rundown of a global crisis. *Infect Drug Resist*. 2018;11:1645–1658. doi:10.2147/IDR.S173867
16. Gounani Z, Asadollahi MA, Pedersen JN, et al. Mesoporous silica nanoparticles carrying multiple antibiotics provide enhanced synergistic effect and improved biocompatibility. *Colloid Surface B*. 2019;175:498–508. doi:10.1016/j.colsurfb.2018.12.035
17. Reyes-Torres MA, Mendoza-Mendoza E, Miranda-Hernández ÁM, et al. Synthesis of CuO and ZnO nanoparticles by a novel green route: antimicrobial activity, cytotoxic effects and their synergism with ampicillin. *Ceramics Int*. 2019;45(18):24461–24468. doi:10.1016/j.ceramint.2019.08.171
18. Nishanthi R, Malathi S, Palani P. Green synthesis and characterization of bioinspired silver, gold and platinum nanoparticles and evaluation of their synergistic antibacterial activity after combining with different classes of antibiotics. *Mater Sci Eng*. 2019;96:693–7[illegible]. doi:10.1016/j.msec.2018.11.050
19. Ahmad S, Hameed A, Khan K, et al. Evaluation of synergistic effect of nanoparticles with antibiotics against enteric pat[illegible] *Appl Nanosci*. 2019;1–4.
20. Ong TH, Chitra E, Ramamurthy S, Ling CCS, A[illegible]bu SP, D[illegible]amani F. Cationic chitosan-propolis nanoparticles alter t[illegible]eta [illegible] S. epidermidis, inhibit biofilm formation b[illegible]modulat[illegible]ene expression and exhibit synergism with antib[illegible]s. *PLoS One*. 2019;14:2. doi:10.1371/journal.pone.0213079
21. Wypij M, Czarnecka J, Świecimska M, Dahm[illegible] Rai M, Golinska P. Synthesis, characterization an[illegible]valuation of anti[illegible]crobial and cytotoxic activities of biogen[illegible] silver nanoparticles s[illegible]thesized from Streptomyces xinghai[illegible]s OF1 strain. *World J Microbiol Biotechnol*. 2018;34(2):2[illegible]9. d[illegible]10.1007/s11274-017-2406-3
22. Panáček A, Smé[illegible]á M, [illegible]anová M[illegible]et al. Strong and nonspecific syner[illegible]tic a[illegible]bacteria[illegible]ffici[illegible]cy of antibiotics combined with silve[illegible]nanopart[illegible]es at ve[illegible]low concentrations showing no cyto[illegible]c effe[illegible]*ules*. 2016;21(1):26. doi:10.3390/molecules21[illegible]
23. Asghar MA, Y[illegible]uf RI, Shoaib MH, Asghar MA. Antibacterial, anticoagulant and c[illegible]toxic evaluation of biocompatible nanocomposite of chitosan loaded green synthesized bioinspired silver nanoparticles. *Int J Biol Macromol*. 2020;160:934–943. doi:10.1016/j.ijbiomac.2020.05.197
24. Kalita S, Kandimalla R, Sharma KK, Kataki AC, Deka M, Kotoky J. Amoxicillin functionalized gold nanoparticles reverts MRSA resistance. *Mater Sci Eng*. 2016;61:720–727. doi:10.1016/j.msec.2015.12.078
25. Harshiny M, Matheswaran M, Arthanareeswaran G, Kumaran S, Rajasree S. Enhancement of antibacterial properties of silver nanoparticles–ceftriaxone conjugate through Mukia maderaspatana leaf extract mediated synthesis. *Ecotoxicol Environ Saf*. 2015;121:135–141. doi:10.1016/j.ecoenv.2015.04.041
26. Deng H, McShan D, Zhang Y, et al. Mechanistic study of the synergistic antibacterial activity of combined silver nanoparticles and common antibiotics. *Environ Sci Technol*. 2016;50(16):8840–8848. doi:10.1021/acs.est.6b00998
27. Khan MN, Lin H, Li M, et al. Identification and growth optimization of a Marine Bacillus DK1-SA11 having potential of producing broad spectrum antimicrobial compounds. *Pak J Pharm Sci*. 2017;30(3):839–853.
28. Turlej-Rogacka A, Xavier BB, Janssens L, et al. Evaluation of colistin stability in agar and comparison of four methods for MIC testing of colistin. *Eur J Clin Microbiol Infect Dis*. 2018;37(2):345–353. doi:10.1007/s10096-017-3140-3
29. Doern CD. When does 2 plus 2 equal 5? A review of antimicrobial synergy testing. *J Clin Microbiol*. 2014;52(12):4124–4128. doi:10.1128/JCM.01121-14
30. Shafiq Y, Naqvi SBS, Rizwani GH, [illegible]al. Asse[illegible]ent of killing kinetics assay and bactericidal mech[illegible]sm of crude m[illegible]hanolic bark extract of Casuarina equisetifolia. [illegible] *J Pharm [illegible]*. 2018;31(5):2143–2148.
31. Mazur P, Skiba-Kurek I, [illegible]rowiec P, Kar[illegible]wsk[illegible]E, Drożdż R. Synergistic ROS-associ[illegible] antimic[illegible]ial activi[illegible]f silver nanoparticles and gentamicin a[illegible]nst [illegible]phylococcus epidermidis. *Int J Nanomed*. 2020;1[illegible]551–35[illegible]oi:10.214[illegible]JN.S246484
32. Müller G, Kra[illegible] A. Biocomp[illegible]ility [illegible]dex of antiseptic agents by parallel ass[illegible]nen[illegible]f antimicrobia[illegible]ivity and cellular cytotoxicity. *J Antimicrob Chem[illegible]r*. 2008;61(6):1281–1287. doi:10.1093/jac/dkn12[illegible]
33. R[illegible]han AA, Riaz A, Asgh[illegible] MA, Raza ML, Ahmed S, Khan K. In [illegible]o assessment of anticoagulant and antiplatelet effects of Syzygium [illegible]mini leaves e[illegible]act in rabbits. *BMC Complement Altern Med*. 2[illegible]9:19(1):236. [illegible]:10.1186/s12906-019-2661-y
34. Rec[illegible]ati C, D[illegible] Maglie M, Bianchessi S, et al. Tissue distribution and acute [illegible]icity of silver after single intravenous administration in [illegible] nano-specific and size-dependent effects. *Particle Fibre Toxicol*. 2015;13(1):12. doi:10.1186/s12989-016-0124-x
35. Close MB, Banister K, Baumans V, et al. Recommendations for euthanasia of experimental animals: part. *Lab Anim*. 1996;30:293–316. doi:10.1258/002367796780739871
36. Oecd. *OECD Guidelines for the Testing of Chemicals*. Organization for Economic; 1994.
37. Lee JH, Kim YS, Song KS, et al. Biopersistence of silver nanoparticles in tissues from Sprague–Dawley rats. *Particle Fibre Toxicol*. 2013;10(1):36. doi:10.1186/1743-8977-10-36
38. Magaye RR, Yue X, Zou B, et al. Acute toxicity of nickel nanoparticles in rats after intravenous injection. *Int J Nanomed*. 2014;9:1393–1402.
39. Rojanarata T, Opanasopit P, Ngawhirunpat T, Saehuan C, Wiyakrutta S, Meevootisom V. A simple, sensitive and green bienzymatic UV-spectrophotometric assay of amoxicillin formulations. *Enzyme Microbial Technol*. 2010;46(34):292–296. doi:10.1016/j.enzmictec.2009.11.011
40. Attimarad M, Al-Dhubiab BE, Alhaider IA, Nair AB. Simultaneous determination of moxifloxacin and cefixime by first and ratio first derivative ultraviolet spectrophotometry. *Chem Cent J*. 2012;6(1):105. doi:10.1186/1752-153X-6-105
41. Maleque M, Hasan MR, Hossen F, Safi S. Development and validation of a simple UV spectrophotometric method for the determination of levofloxacin both in bulk and marketed dosage formulations. *J Pharm Anal*. 2012;2(6):454–457. doi:10.1016/j.jpha.2012.06.004
42. Asghar MA, Zahir E, Shahid SM, et al. Iron, copper and silver nanoparticles: green synthesis using green and black tea leaves extracts and evaluation of antibacterial, antifungal and aflatoxin B1 adsorption activity. *LWT*. 2018;90:98–107. doi:10.1016/j.lwt.2017.12.009
43. Homayoonfal M, Mehrnia MR. Amoxicillin separation from pharmaceutical solution by pH sensitive nanofiltration membranes. *Sep Purif Technol*. 2014;130:74–83. doi:10.1016/j.seppur.2014.04.009

44. Mishra B, Singh AK, Yadav SK. Study of comparative aspects of gastroretentive delivery of cefixime trihydrate from microspheres and microsphere based tablets. *J Pharm Invest*. 2015;45(6):541–554. doi:10.1007/s40005-015-0202-3
45. Khan G, Yadav SK, Patel RR, Nath G, Bansal M, Mishra B. Development and evaluation of biodegradable chitosan films of metronidazole and levofloxacin for the management of periodontitis. *AAPS Pharmscitech*. 2016;17(6):1312–1325. doi:10.1208/s12249-015-0466-y
46. Jyoti K, Baunthiyal M, Singh A. Characterization of silver nanoparticles synthesized using Urtica dioica Linn. leaves and their synergistic effects with antibiotics. *J Rad Res Appl Sci*. 2016;9(3):217–227.
47. Reidy B, Haase A, Luch A, Dawson KA, Lynch I. Mechanisms of silver nanoparticle release, transformation and toxicity: a critical review of current knowledge and recommendations for future studies and applications. *Mater*. 2013;6(6):2295–2350. doi:10.3390/ma6062295
48. Rai M, Deshmukh S, Ingle A, Gade A. Silver nanoparticles: the powerful nanoweapon against multidrug-resistant bacteria. *J Appl Microbiol*. 2012;112(5):841–852. doi:10.1111/j.1365-2672.2012.05253.x
49. Kim S-H, Lee H-S, Ryu D-S, Choi S-J, Lee D-S. Antibacterial activity of silver-nanoparticles against Staphylococcus aureus and Escherichia coli. *Korean J Microbiol Biotechnol*. 2011;39(1):77–85.
50. Pellieux C, Dewilde A, Pierlot C, Aubry J-M. Bactericidal and virucidal activities of singlet oxygen generated by thermolysis of naphthalene endoperoxides. *Methods Enzymol*. 2000;319:197–207.
51. Tang R, Yu Z, Zhang Y, Qi C. Synthesis, characterization, and properties of antibacterial dye based on chitosan. *Cellulose*. 2016;23(3):1741–1749. doi:10.1007/s10570-016-0935-9
52. Ali SG, Ansari MA, Khan HM, Jalal M, Mahdi AA, Cameotra SS. Antibacterial and antibiofilm potential of green synthesized silver nanoparticles against imipenem resistant clinical isolates of [illegible]ruginosa. *BioNanoSci*. 2018;8(2):544–553. doi:10.1007/s12668-018-0505-8
53. Dahm H. Silver nanoparticles in wound infections: [illegible]ent status [illegible] future prospects. In: Rai M, editor. *Nanotechnology [illegible] Skin, [illegible] Tissue, and Bone Infections*. Cham: [illegible]pringer [illegible]ternation[illegible] Publishing; 2020:151–168.
54. Alavi M, Rai M. Recent advances i[illegible]antiba[illegible] applications of metal nanoparticles (MNPs) and [illegible]etal nanoc[illegible]posites (MNCs) against multidrug-resistant (MD[illegible]cteria. *Expert [illegible]v Anti-Infect Ther*. 2019;17(6):419–428. do[illegible]0.1080[illegible]1787210.2019.1614914
55. Nakazato G, Lonni AASG, Panagio LA, [illegible]. Applications of nanometals in cutaneous inf[illegible]ions. In: Rai M, ed[illegible] *Nanotechnology in Skin, Soft Tissue, a[illegible] Bone Inf[illegible]ions*. Cham: Springer International Publishing; 2020:[illegible]92.
56. Alavi M, Karimi N. Antiplanktonic, antibiofilm, antiswarming motility and antiquorum sensing activities of green synthesized Ag–TiO2, TiO2–Ag, Ag–Cu and Cu–Ag nanocomposites against multi-drug-resistant bacteria. *Artif Cells Nanomed B*. 2018;46(sup3):S399–S413. doi:10.1080/21691401.2018.1496923
57. Alavi M, Rai M. Recent progress in nanoformulations of silver nanoparticles with cellulose, chitosan, and alginic acid biopolymers for antibacterial applications. *Appl Microbiol Biotechnol*. 2019;103(2122):8669–8676. doi:10.1007/s00253-019-10126-4
58. Hwang I-S, Hwang JH, Choi H, Kim K-J, Lee DG. Synergistic effects between silver nanoparticles and antibiotics and the mechanisms involved. *J Med Microbiol*. 2012;61(12):1719–1726.
59. Vazquez-Muñoz R, Meza-Villezcas A, Fournier P, et al. Enhancement of antibiotics antimicrobial activity due to the silver nanoparticles impact on the cell membrane. *PLoS [illegible]* [illegible]2019;14(11):e0224904. doi:10.1371/journal.pone.0224904
60. Kohanski MA, Dwyer DJ, Ha[illegible]e B, Lawrence [illegible]A, Collins JJ. A common mechanism of cellular d[illegible]th induced by [illegible]bactericidal antibiotics. *Cell*. 2007;130(5[illegible]97–810. d[illegible]10.1016/j[illegible]ell.2007.06.049
61. Kokila T, Ramesh P, [illegible]etha D. Biosyn[illegible]sis [illegible] silver nanoparticles from Cavendish b[illegible]na peel [illegible]tract and [illegible] antibacterial and free radical scavenging a[illegible]y: a [illegible]vel biolo[illegible]al approach. *Appl Nanosci*. 2015;5(8):91[illegible]920. doi:[illegible]1007/s132[illegible]-015-0401-2
62. Zhang W[illegible]Y, Niu J, Ch[illegible]Y. P[illegible]togeneration of reactive oxygen specie[illegible]n un[illegible]ted silver, go[illegible]ickel, and silicon nanoparticles and their antibacteria[illegible]ffects. *Langmuir*. 2013;29(15):4647–4651. doi:10.[illegible]la400500t
[illegible] Xue Y, Zhang S, Hua[illegible]g Y, et al. Acute toxic effects and gender-related biok[illegible]etics of silver nanoparticles following an intravenous injection in [illegible]ce. *J Appl Toxicol*. 2012;32(11):890–899. doi:10.1002/jat.2742
64. [illegible]boud[illegible] Kaplowitz N. Drug-induced liver injury. *Drug Saf*. 2007;30(4):277–294. doi:10.2165/00002018-200730040-00001
[illegible]iannini EG, Testa R, Savarino V. Liver enzyme alteration: a guide for clinicians. *CMAJ*. 2005;172(3):367–379. doi:10.1503/cmaj.1040752
66. Kim YS, Kim JS, Cho HS, et al. Twenty-Eight-Day Oral Toxicity G. Gender-related tissue distribution of silver nanoparticles in Sprague-Dawley rats. *Inhal Toxicol*. 2008;20:575–583. doi:10.1080/08958370701874663
67. Sung JH, Ji JH, Yoon JU, et al. Lung function changes in Sprague-Dawley rats after prolonged inhalation exposure to silver nanoparticles. *Inhal Toxicol*. 2008;20(6):567–574. doi:10.1080/08958370701874671